An introduction to OFDM

Lecture notes in the course Digital communications, advanced course (ETTN01)

Göran Lindell, Version 161115

Section 1: Introduction

The modulation technique referred to as OFDM (Orthogonal Frequency Division Multiplexing) is of particular interest since it is used today in a number of important and high-performing communication systems. Some examples are DVB-T, LTE (4G), WLAN, WIMAX.

An OFDM signal extends over a T_s second long time-interval, which is referred to as the OFDM signal (or symbol) interval. In practice, a new OFDM signal is sent every T_s second, and the value of T_s depends on the application, e.g., $T_s = 1$ ms, or smaller.

An OFDM signal can be described as the sum of K different QAM signals, where all QAM signals use the same T_s-long time-interval. Hence, K QAM signals are *simultaneously* transmitted within the OFDM signal interval. The value of K is typically quite large, several hundred or several thousand. *A large value of K immediately leads to the question how to implement an OFDM signal in practice.* Even if a single QAM-signal is easy to implement (as we will see below), it is neither practical nor economical to implement say 1000 individual QAM-signals, and then add them to create an OFDM signal (every T_s). As we will see there are very elegant engineering solutions to this problem.

The main purpose of these introductory lecture notes is to describe efficient, i.e. very fast and economical, implementations of the OFDM modulator (at the transmitter side) and the OFDM demodulator (at the receiver side). *The importance of efficient implementations should not be under-estimated, since the success of OFDM to a very large extent relies on the fact that efficient implementations exist!*

The transmitter typically consists of a digital part followed by an analog part, where discrete-time and continuous-time operations are performed, respectively, see Figure 1. This figure illustrates the over-all structure and operations performed by an OFDM transmitter within an OFDM symbol interval T_s. Digital-to-Analog (D/A) converters act as interface between the digital domain and the analog domain. In connection to the synthesis of an OFDM signal, the Inverse Discrete Fourier Transform (IDFT) plays a fundamental role in the digital domain while the analog domain typically includes filtering, mixing (frequency up-conversion) and power amplifying (PA) operations. The IDFT, the so-called cyclic prefix (CP), as well as the other operations indicated in Figure 1 will be further explained and clarified as we proceed in these lecture notes. A more detailed example of a transmitter structure is given in Figure 7 and Figure 8 on pages 27 and 31, respectively.

| Create K QAM symbols from coded bits. Create the size-N input sequence to the IDFT. | Calculate the size-N output sequence from the IDFT. | Append the size-L CP to the beginning of the IDFT output sequence, resulting in a size (L+N) sequence. | Perform D/A conversion to produce continuous-time signals from discrete-time signals. | Frequency up-conversion. Power amplifier. Antenna coupling unit. |

Discrete-time operations   Continuous-time operations

Figure 1. Illustrates the over-all structure and operations performed by an OFDM transmitter within an OFDM symbol interval T_s.

| Antenna coupling unit. Bandpass (BP) filter. Low-noise amplifier (LNA). Frequency down-conversion. | Perform A/D conversion to produce discrete-time signals from continuous-time signals. Lr+Nr samples are obtained. | Remove the Lr samples that correspond to the CP. This results in a size-Nr input sequence to the DFT. | Calculate the size-Nr output sequence from the DFT. | Extract the K distorted and noisy QAM signal points. | Decoding unit. This results in the sequence of decoded information bits. |

Continuous-time operations   Discrete-time operations

Figure 2. Illustrates the over-all structure and operations performed by an OFDM receiver within an OFDM symbol interval T_s.

The received signal is a distorted and noisy version of the transmitted analog OFDM signal. The receiver typically consists of an analog part followed by a digital part, where continuous-time and discrete-time operations are performed, respectively, see Figure 2. This figure illustrates the over-all structure and operations performed by an OFDM receiver within an OFDM symbol interval T_s. Analog-to-Digital (A/D) converters act as interface between the analog domain and the digital domain. The analog domain of the receiver typically includes filtering, amplifying and mixing (frequency down-conversion) operations, while the Discrete Fourier Transform (DFT) plays a fundamental role in the digital domain. The values of the two parameters denoted Lr and Nr in Figure 2 depend on the sampling frequency used in the receiver, and these two values do not need to be the same as the values of the corresponding parameters L and N at the transmitter side in Figure 1. The DFT, as well as the

other operations indicated in Figure 2 will be further explained and clarified as we proceed in these lecture notes. A more detailed example of a receiver structure is given in Figure 10 and Figure 11 on pages 38 and 42, respectively. It should also be mentioned here that the decoding unit in Figure 2 may need to use several size-K input vectors, corresponding to several OFDM intervals, until the entire original sequence of information bits can be decoded.

The physical communication link (or channel) is analog. Hence, the complete communication chain transmitter-channel-receiver consists of a mixture of digital and analog operations. More details about these operations will be given as we continue in these lecture notes.

The literature on different aspects of OFDM is extensive and the reader is strongly recommended to investigate, e.g., the important database IEEE Xplore [http://ieeexplore.ieee.org/Xplore/DynWel.jsp] to acquire information of recent advances related to OFDM, as well as tutorials. As examples of books that contain descriptions and/or applications of OFDM we have refs. [2]-[11].

Each of the K QAM signals that constitute the OFDM signal has a different carrier frequency, which we refer to as a **sub-carrier frequency**. The choice of sub-carrier frequencies in OFDM is such that the frequency separation between neighboring sub-carriers is always equal to f_Δ Hz. How to choose f_Δ will be explained in detail in the next section. The value of f_Δ depends on the application.

Let us number the K QAM signals from 0 up to K-1 according to increasing sub-carrier frequency. Then we have that the QAM signal with index k has the sub-carrier frequency f_k Hz,

$$f_k = f_0 + k f_\Delta, \quad k = 0,1,\dots,K-1 \tag{1.1}$$

The choice of *the overall carrier frequency* f_c is in principle arbitrary, but here we define f_c as the center frequency in the OFDM frequency band, i.e.,

$$f_c = f_0 + \frac{K-1}{2} f_\Delta \tag{1.2}$$

It is seen in Equation (1.2) that if K is an odd number then f_c coincide with the sub-carrier frequency $f_{(K-1)/2}$. On the other hand, if K is an even number then f_c is exactly in the middle between the two sub-carrier frequencies $f_{(K-2)/2}$ and $f_{K/2}$. In, e.g., LTE-applications the overall carrier frequency f_c typically is in the GHz range, and K is an odd number in the down-link while K is an even number in the up-link [9].

From Equation (1.1) the **bandwidth** of the OFDM signal is found to be approximately $(K+1)f_\Delta$ Hz (here we have also taken into consideration the bandwidth consumption f_Δ at the two edges of the frequency band). In these lecture notes K is typically $\gg 1$, and then the bandwidth, here denoted W_{OFDM}, of the OFDM signal is approximately $K f_\Delta$ Hz, i.e.

$$W_{OFDM} \approx K f_\Delta \text{ (Hz)} \tag{1.3}$$

Let us now take a closer look at the QAM signal with index k, within the time-interval $0 \leq t \leq T_s$ where it can be expressed as,

$$g_{rec}(t)\big(a_{k,I}\cos(2\pi f_k t) - a_{k,Q}\sin(2\pi f_k t)\big) = g_{rec}(t)Re\{a_k e^{j2\pi f_k t}\} \qquad (1.4)$$

The left-hand side above is the conventional so-called I/Q description of a QAM signal. The pulse $g_{rec}(t)$ is a rectangular pulse equal to a constant value within the time-interval $0 \leq t \leq T_s$, and it equals zero outside this time-interval. The *information* is carried by the pair $(a_{k,I}, a_{k,Q})$ of values, and there are M_k unique pairs. Each pair is usually referred to as a **signal point**. The size of the QAM *signal constellation* with index k is denoted M_k and it is typically a power of 4 (4, 16, 64, 256,…).

The right-hand side in Equation (1.4) is also a conventional description of a QAM-signal, and it uses **complex notation**. *Observe that this description will be used almost exclusively in these lecture notes!* In Equation (1.4) the complex number a_k is defined as,

$$a_k = a_{k,I} + j a_{k,Q}, \quad k = 0,1, \dots, K-1 \qquad (1.5)$$

where $a_{k,I}$ and $a_{k,Q}$ are the real part and the imaginary part of a_k, respectively. Hence, *in this description the information is contained in the complex number a_k* (which also is referred to as a **signal point**). *It is very important to understand that the two QAM-descriptions given in Equation (1.4) are identical!*

Due to the rectangular pulse shape, the Fourier transform of the QAM signal in Equation (1.4) is **sinc-shaped** around the sub-carrier frequency f_k, with **peak absolute value** at $f = f_k$, and it has **zero-crossings** at the frequencies $f = f_k + i/T_s$ (for any non-zero integer i). Hence, the width of the **main-lobe** is $2/T_s$ Hz.

We need a suitable description of the OFDM signal. By this is meant a description that is tailored to the modeling and implementation issues considered in these lecture notes. As will be more clear in section 2, it is convenient to introduce a so-called *reference* carrier frequency, denoted f_{rc}, chosen to be one of the sub-carrier frequencies closest to the overall carrier frequency f_c. Based on the discussion in connection to Equation (1.2), the ***reference carrier frequency*** f_{rc} is defined by,

$$f_{rc} = f_c = f_{(K-1)/2} \qquad \text{if K is odd} \qquad (1.6)$$

$$f_{rc} = f_c - f_\Delta/2 = f_{(K-2)/2} \qquad \text{if K is even} \qquad (1.7)$$

Furthermore, now we can express sub-carrier frequency f_k by using f_{rc} as a reference in the following useful way,

$$f_k = f_{rc} + g_k f_\Delta, \quad k = 0,1, \dots, K-1 \qquad (1.8)$$

and this will be used a lot in section 2 where a *baseband* (low-frequency) version of the OFDM signal is investigated. The number g_k in Equation (1.8) denotes an integer value defined by,

$$g_k = g_0 + k = k - k_{rc} = k - (K-1)/2 \quad \text{if K is odd} \qquad (1.9)$$

$$g_k = g_0 + k = k - k_{rc} = k - (K-2)/2 \quad \text{if K is even} \qquad (1.10)$$

where k_{rc} denotes the value of k corresponding to f_{rc}, see Equations (1.6)-(1.7). As will be seen in section 2, g_k is an alternative very useful way of numbering the corresponding K *baseband* sub-carrier frequencies. The parameter k in Equation (1.1) numbers the sub-carrier frequencies from 0 to K-1, but g_k in Equation (1.8) instead numbers the sub-carrier frequencies *relative* to the reference carrier frequency f_{rc}. It is also seen in Equations (1.8)-(1.10) that $g_0 = -k_{rc}$ and that $g_k = 0$ corresponds to the sub-carrier number $k = k_{rc}$ of the reference carrier frequency f_{rc}, i.e. $g_{k_{rc}} = 0$.

The numbers g_k range from g_0 to g_{K-1},

$$g_k: -\frac{K-1}{2} = g_0, \dots, -1, 0, 1, \dots, \frac{K-1}{2} = g_{K-1} \quad \text{if K is odd} \tag{1.11}$$

$$g_k: -\frac{K-2}{2} = g_0, \dots, -1, 0, 1, \dots, \frac{K}{2} = g_{K-1} \quad \text{if K is even} \tag{1.12}$$

Examples: If K=8 then $g_0 = -3$, $g_3 = 0$ and $g_7 = 4$. If K=9 then $g_0 = -4$, $g_4 = 0$ and $g_8 = 4$.

By extending Equation (1.4) to describe the sum of K QAM signals, and also use the expression in Equation (1.8), i.e., $f_k = f_{rc} + g_k f_\Delta$, $k = 0, 1, \dots, (K-1)$, **a compact expression of an OFDM signal** in the time-interval $0 \leq t \leq T_s$ is obtained as,

OFDM signal(t) $= g_{rec}(t) \sum_{k=0}^{K-1} Re\{a_k e^{j2\pi f_k t}\} = g_{rec}(t) Re\{\sum_{k=0}^{K-1} a_k e^{j2\pi f_k t}\} =$

$= g_{rec}(t) Re\{\sum_{k=0}^{K-1} a_k e^{j2\pi(f_0 + k f_\Delta)t}\} = g_{rec}(t) Re\{(\sum_{k=0}^{K-1} a_k e^{j2\pi(g_0 + k)f_\Delta t}) e^{j2\pi f_{rc} t}\} =$

$= g_{rec}(t) Re\{(\sum_{k=0}^{K-1} a_k e^{j2\pi g_k f_\Delta t}) e^{j2\pi f_{rc} t}\}$ (1.13)

Equation (1.13) shows that an OFDM signal can be viewed as the sum of K QAM signals, and this is the most basic characteristics of an OFDM signal. It is also seen that an OFDM signal can be expressed in several ways. The last expression in Equation (1.13) will be used extensively in the next sections since this expression is a suitable starting point to find an efficient implementation of the OFDM signal.

Let us now, as an example, take a closer look at Equation (1.13) for the special case when K is odd. In this case the OFDM signal in Equation (1.13) can be expressed as,

OFDM signal(t) $= = g_{rec}(t) Re\{(\sum_{k=0}^{K-1} a_k e^{j2\pi(-(K-1)/2 + k)f_\Delta t}) e^{j2\pi f_c t}\} =$

$= g_{rec}(t) Re\left\{(\sum_{l=-(K-1)/2}^{(K-1)/2} a_{l+(K-1)/2} e^{j2\pi l f_\Delta t}) e^{j2\pi f_c t}\right\}$, if K is odd (1.14)

In a similar way we obtain from Equation (1.13) that for the special case when K is even, the OFDM signal can be expressed as,

OFDM signal(t) $= = g_{rec}(t) Re\{(\sum_{k=0}^{K-1} a_k e^{j2\pi(-(K-2)/2 + k)f_\Delta t}) e^{j2\pi f_{rc} t}\} =$

$= g_{rec}(t) Re\left\{(\sum_{l=-(K-2)/2}^{K/2} a_{l+(K-2)/2} e^{j2\pi l f_\Delta t}) e^{j2\pi f_{rc} t}\right\}$, if K is even (1.15)

Figure 3a on page 10 shows an example if $K = 8$, and this figure roughly indicates some frequency-domain properties of an OFDM signal. Figure 3a illustrates the main-lobes of the eight individual QAM-signals that constitute the OFDM signal. The side-lobes of each QAM-signal are, however, **not** shown in Figure 3a.

For the moment we do not know how to efficiently create an OFDM signal in practice if K is large. As will be seen in section 2, the last expression in Equation (1.13) is indeed very useful to find an efficient implementation. Observe that both the numbering g_k and the reference carrier frequency f_{rc} are present in Equation (1.13).

The number of **coded bits** carried by the OFDM signal in Equation (1.13) is denoted B_c, and $B_c = \sum_{k=0}^{K-1} log_2(M_k)$. The coded bits are here assumed to be the output coded bits from a single encoder. The corresponding input bits to the encoder are the **information bits**, and we here assume that B_i information bits generate B_c coded bits. Hence, the code rate of the encoder, denoted r_c, therefore is $r_c = B_i/B_c$ (information bit per coded bit).

The transmitted **information bit rate**, denoted R_b, then equals,

$$R_b = \frac{r_c \sum_{k=0}^{K-1} log_2(M_k)}{T_s} \text{ (bps)} \tag{1.16}$$

Furthermore, assuming also that K is $\gg$ 1 the **bandwidth efficiency**, denoted ρ, is

$$\rho = \frac{R_b}{W_{OFDM}} = \frac{r_c \sum_{k=0}^{K-1} log_2(M_k)}{T_s K f_\Delta} \text{ (bps/Hz)} \tag{1.17}$$

As an **example**: If $r_c = 3/4$, K=600, $f_\Delta = 11000\ Hz$, and if 64-QAM is used throughout, then 3600 coded bits are sent every T_s. Furthermore, if $T_s = 0.1$ ms then $R_b = 27$ Mbps and $\rho = 4.09$ bps/Hz.

In case of **uncoded**, (i.e. $r_c = 1$) OFDM, though seldom used in practice, and if $M_n = M$, then it is found from the above that the information bit rate equals $K\ log_2(M)/T_s$ bps and this implies that the bandwidth efficiency then equals $\frac{log_2(M)}{T_s f_\Delta}$ bps/Hz.

The communication channel is assumed to be a **multi-path channel**. Such a channel typically distorts the transmitted OFDM signal such that, e.g., in the beginning of the OFDM symbol interval *an initial relatively short transient* behavior of the signal occurs. This will be described in detail in Section 5.

The first part of the transmitted OFDM signal is referred to as the **Cyclic Prefix** (CP) and its duration is denoted T_{CP}. In most cases $T_{CP} \ll T_s$. The main purpose of the CP is that the initial transient behavior of the multi-path channel <u>output</u> signal should occur within the duration of the CP. In a sense, the CP acts as a "guard interval" in the time-domain.

The CP plays an important role at the receiver side since, as we will see in Sections 5-6, it is possible to completely eliminate interference between OFDM signals provided that the CP is properly chosen. Hence, as long as the CP is properly chosen, such *inter-symbol interference (ISI)* between OFDM signals will **not** be present in the receiver, and that is a major advantage of OFDM. More details about the CP will be given in Sections 3,5,6.

The remaining part of the OFDM signal interval is referred to as **the receiver's observation interval** and its duration is denoted T_{obs},

$$T_{obs} = T_s - T_{CP} \tag{1.18}$$

The receiver's observation interval is the time-interval of the received signal that the receiver uses for extraction of the K received distorted and noisy signal points (which in turn are used by the decoding unit in Figure 2). Hence, for efficient operation this time interval should constitute the major part of

the OFDM symbol time T_s, i.e. $T_{CP} \ll T_s$, since otherwise too much signal power is spent on a signal (the CP) that actually will not be used in the detection process in the receiver. Observe also from Equations (1.16) and (1.18) that T_{CP} enters into the expression for the information bit rate R_b.

Let us here also briefly introduce the concept of **the OFDM time-frequency grid** (see, e.g., ref. [9]). This concept is usually clarified by a figure that has the K consecutive sub-carrier frequencies on the vertical axis, and say P consecutive OFDM symbol intervals on the horizontal axis. This kind of figure gives a very useful overview of the over-all communication resources within the time-interval PT_s (second). The overall communication resources above equal KP so-called **resource units**, corresponding to KP information carrying QAM signal points.

As an example: Let us consider LTE-systems (Long-Term Evolution). In LTE (from ref. [9]), OFDM is used and $f_\Delta = \frac{1}{T_{obs}} = 15$ kHz (which means that $T_{obs} = 66.67$ μs, see Equation (2.1) in section 2). A typical OFDM symbol interval T_s in LTE is 71.36 μs, and 14 consecutive OFDM signals are then generated every ms. Furthermore, a so-called **resource block** in LTE typically consists of 12 consecutive sub-carrier frequencies (covering 180 kHz) and 7 consecutive OFDM symbol intervals (covering 0.5 ms). Hence, such a resource block contains 84 resource units (i.e. 84 QAM signal points). Within a 20 Mhz bandwidth typically 110 such resource blocks are defined, covering 19.8 MHz and corresponding to K=1320.

As an **example**: Let us consider the WLAN standard IEEE 802.11n (see ref. [11]). In this system OFDM is used with K=117, $f_\Delta = 312.5$ kHz and $T_s = 4$ μs (normal). Of the 117 subcarriers, the 3 center subcarriers are set to zero, 108 subcarriers are used for data transmission, and 6 subcarriers are used as pilots. In case of $r_c = 5/6$, and 64-QAM on each of the 108 subcarriers, the information bit rate equals 135 Mbps (see Equation (1.16). Furthermore, for this scheme $W_{OFDM} \approx 36.6$ MHz (the nominal bandwidth is 40 MHz).

For future reference we here also give the definition of ***orthogonal signals***. Two real or complex signals $s(t)$ and $z(t)$ are orthogonal over the time-interval $t_1 \leq t \leq t_2$ if and only if,

$$\int_{t_1}^{t_2} s(t)z^*(t) \, dt = 0 \tag{1.19}$$

where the symbol * denotes conjugate.

The structure of these lecture notes is quite similar to the order of the operations indicated in Figure 1 and in Figure 2. *A short summary of some basic relationships* is given at several places in these lecture notes to make it easier to identify and locate important concepts and results.

The last part of this introduction is a compact overview of the remaining sections in these lecture notes.

Section 2:

- How to obtain N **time-domain complex samples** of a complex baseband (low-frequency) OFDM signal by using the size-N **IDFT** (Inverse Discrete Fourier Transform).

Section 3:

- By adding L **additional** time-domain complex samples, corresponding to the **CP** (Cyclic Prefix), a new size-(L+N) sequence of complex samples is constructed
- By using **D/A converters**, applied to the size-(L+N) complex sequence, the continuous-time (analog) **I- and Q-components** of the desired OFDM signal are created.

Section 4:

- By I/Q frequency up-conversion (mixing) to the carrier frequency and power amplifying **the desired transmitted OFDM signal** is created.

Section 5:

- How the OFDM signal is **changed** by the channel (H(f) and AWGN).

Section 6:

- Frequency down-conversion to baseband at the receiver side and **extracting the information carrying I- and Q-components** of the received distorted and noisy OFDM signal.
- **Sampling** the received I- and Q-components (**A/D conversion**), and **removal of the CP**.
- Using the size-N **DFT** (Discrete Fourier Transform) to obtain **the K received distorted and noisy signal points**.

Section 7:

- An **alternative transmitter** implementation (among several). If the same K and f_Δ as in sections 2-4 are used, then this alternative implementation requires a higher sampling frequency. The description given here is to a large extent influenced by the description in ref. [2].

Section 8:

- An **alternative receiver** implementation (among several). If the same K and f_Δ as in section 6 are used, then this alternative implementation requires a higher sampling frequency.

Section 2: A sampled version of a T_{obs}-long baseband OFDM signal

Our goal in this section is to use the size-N IDFT (Inverse Discrete Fourier transform) to efficiently create N time-domain complex samples of a complex baseband OFDM signal, within the time-interval $0 \le t \le T_{obs}$. *Observe however* that these N samples will in Section 3 be time-shifted T_{CP} seconds to obtain the samples of the desired OFDM signal within the time-interval $T_{CP} \le t \le T_s$.

In Section 3 we will also add the CP by adding L additional samples to the already created N samples, and the L samples correspond to the time-interval $0 \le t \le T_{CP}$. As will be seen, the CP is constructed by adding a so-called *periodic extension* of the N samples. In this way all $L + N$ samples of a complex baseband OFDM signal, within the time-interval $0 \le t \le T_s$, is obtained. The remaining steps are then D/A converters (also in Section 3) and frequency up-conversion (in Section 4).

As was mentioned earlier the receiver´s observation interval constitutes the major part of the OFDM signal interval T_s. Hence the OFDM signal construction within the interval $T_{CP} \le t \le T_s$ is of course important.

The **sub-carrier frequency separation** f_Δ is a fundamental parameter in OFDM and it should be chosen such that,

$$f_\Delta = 1/T_{obs} \qquad (2.1)$$

Among other advantages, this choice makes it possible for all K *received* QAM signals in the received OFDM signal to be **orthogonal over the receiver´s observation interval** (see Equation (1.19)), and this is a fundamental desired property of an OFDM signal. Note however that the requirement in Equation (2.1) assumes an overall *rectangular* pulse within T_{obs}, otherwise all K received QAM signals will not be orthogonal.

Step 1: The equivalent complex baseband signal of a T_{obs}-long OFDM signal .

We now use the same kind of description as in Equation (1.13) to describe an OFDM signal within the time-interval $0 \le t \le T_{obs}$, here denoted $y(t)$,

$$y(t) = Re\{(\textstyle\sum_{k=0}^{K-1} a_k e^{j2\pi g_k f_\Delta t})e^{j2\pi f_{rc}t}\} = Re\{x(t)e^{j2\pi f_{rc}t}\} \qquad (2.2)$$

where

$$x(t) = x_{Re}(t) + jx_{Im}(t) = \textstyle\sum_{k=0}^{K-1} a_k e^{j2\pi g_k f_\Delta t}, \qquad 0 \le t \le T_{obs} \qquad (2.3)$$

and $x(t) = 0$ outside this interval. Observe that the signal $x(t)$ does not contain any high-frequency components, it contains frequency components around the so-called *equivalent baseband sub-carrier frequencies*:

$$g_0 f_\Delta, \dots, -f_\Delta, 0, f_\Delta, \dots\dots, g_{K-1} f_\Delta \qquad (2.4)$$

where g_k is defined in Equations (1.9)-(1.10). Consequently, the signal $x(t)$ contains only *baseband frequencies* (low frequencies) and $x(t)$ is referred to as the *equivalent complex baseband signal* of the OFDM signal y(t). **Note** that for the two cases K odd and K even, explicit expressions of the signal $x(t)$ in Equation (2.3) can be identified in Equations (1.14)-(1.15).

Observe in Equation (2.3) that the QAM symbol a_k (k=0,1,…,(K-1)), is carried by *the baseband sub-carrier frequency $g_k f_\Delta$ in the complex baseband OFDM signal $x(t)$*!

The frequency contents of the signals y(t) and x(t), denoted $Y(f)$ and $X_a(f)$, respectively, are roughly indicated in Figure 3 below for an example where K=8. It is seen in Figure 3a that the high-frequency OFDM signal y(t) carries the QAM-symbols $a_0, a_1, \ldots, a_7$ at the high-frequency sub-carrier frequencies $f_0, f_1, \ldots, f_7$, respectively. For the specific example shown in Figure 3a it is concluded that $|a_7|$ is much larger than $|a_0|$, since the main-lobe around f_7 is much higher than the main-lobe around f_0.

Figure 3b shows the corresponding baseband situation where the complex baseband OFDM signal $x(t)$ carries the QAM-symbols $a_0, a_1, \ldots, a_7$ at the **baseband** sub-carrier frequencies $-3f_\Delta, -2f_\Delta, \ldots, 4 f_\Delta$, respectively (according to Equation (2.4)).
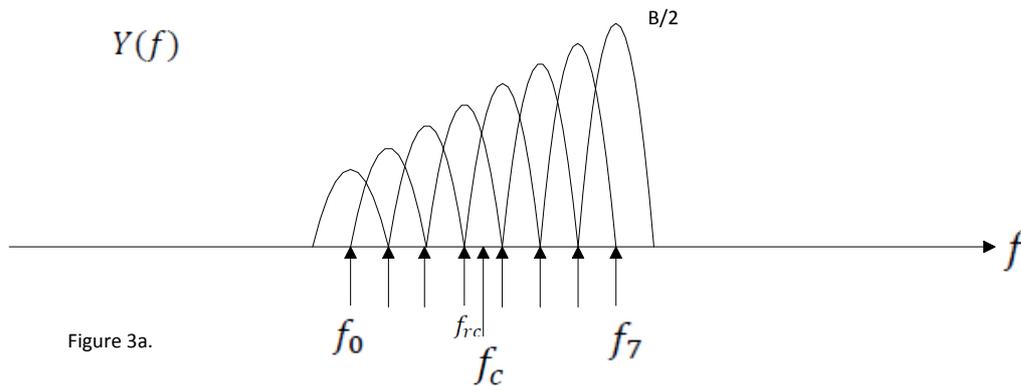
Figure 3a.
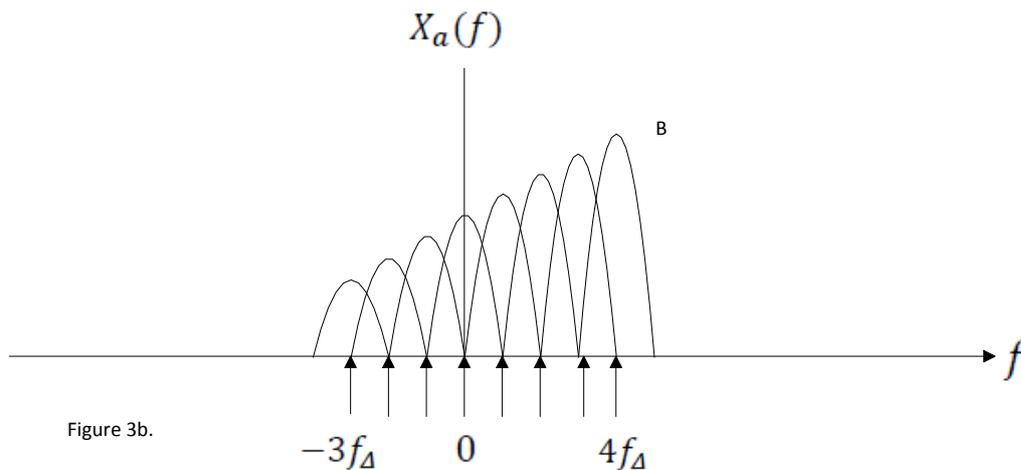
Figure 3b.

Figure 3a) A specific example where $K = 8$, illustrating the main-lobes of the eight individual QAM signals that constitute the OFDM signal $y(t)$ in Equation (2.2). The side-lobes of each QAM-signal are, however, **not** shown in this figure. The Fourier transform $Y(f)$ of the OFDM signal $y(t)$ is only roughly indicated by this figure. The short arrows show the eight sub-carrier frequencies. Furthermore, $f_{rc} = f_3$ in this case. In this example it is also assumed that the specific set of K signal points to be transmitted are such that $|a_0| < |a_1| < |a_2| < \cdots < |a_6| < |a_7|$.
Figure 3b) The baseband version of Figure 3a is here considered. Illustrating the main-lobes for the eight individual complex *baseband* QAM signals that constitute the complex baseband OFDM signal $x(t)$ in Equation (2.3). The Fourier transform $X_a(f)$ of the complex baseband OFDM signal $x(t)$ is only roughly indicated by this figure. The arrows show the 8 *baseband* sub-carrier frequencies.

The high-frequency OFDM signal $y(t)$ in Equation (2.2) can be written as,

$$y(t) = Re\{x(t)e^{j2\pi f_{rc}t}\} = x_{Re}(t)\cos(2\pi f_{rc}t) - x_{Im}(t)\sin(2\pi f_{rc}t) \qquad (2.5)$$

Equation (2.5) is an important relationship since it shows that the OFDM-signal $y(t)$ is **easily implemented** as soon as we have created the real part $x_{Re}(t)$ and the imaginary part $x_{Im}(t)$ of $x(t)$.

We should therefore focus on creating $x(t)$, since $x_{Re}(t)$ and $x_{Im}(t)$ then are easy to find.

Let us first however investigate the Fourier transforms $Y(f)$ and $X_a(f)$ in some more detail. We know that $X_a(f)$ denotes the Fourier transform of the complex baseband OFDM signal $x(t)$. The Fourier transform of the signal $x(t)e^{j2\pi f_{rc}t}$ that appears in Equation (2.5) then is,

$$\int_{-\infty}^{\infty} x(t)e^{j2\pi f_{rc}t}e^{-j2\pi ft}\,dt = X_a(f - f_{rc}) \qquad (2.6)$$

and this is a pure frequency shift of $X_a(f)$. In general, the signal $x(t)e^{j2\pi f_{rc}t}$ is a complex signal and for such signals the Fourier transform does not possess symmetry properties around the frequency $f = 0$. However, the high-frequency OFDM signal $y(t)$ is real, and its Fourier transform $Y(f)$ can be shown to be,

$$Y(f) = (X_a(f - f_{rc}) + X_a^*(-(f + f_{rc})))/2 \qquad (2.7)$$

$Y(f)$ (at positive frequencies only) and $X_a(f)$ are roughly indicated in Figure 3. Symmetry exists in $Y(f)$ since, e.g., $|Y(f)| = |Y(-f)|$. The symbol * denotes conjugate.

It is of great importance to understand the frequency content in the complex baseband OFDM signal $x(t)$. As is seen in Equation (2.3) the signal $x(t)$ is the sum of K complex baseband QAM signals. Let us denote these K individual complex baseband QAM signals by,

$$x_k(t) = a_k e^{j2\pi g_k f_\Delta t}, \quad k = 0,1,\dots,(K-1) \qquad (2.8)$$

where each signal is zero outside the time-interval $0 \le t \le T_{obs}$. The frequency content in the signal $x_k(t)$ is denoted $X_{a,k}(f)$ and

$$X_{a,k}(f) = a_k T_{obs}\frac{sin(\pi(f-f_{x,k})T_{obs})}{\pi(f-f_{x,k})T_{obs}}e^{-j\pi(f-f_{x,k})T_{obs}} \qquad (2.9)$$

where

$$f_{x,k} = g_k f_\Delta = \frac{g_k}{T_{obs}} \qquad (2.10)$$

is the baseband sub-carrier frequency of the signal $x_k(t)$. It is seen in Equation (2.9) that the Fourier transform of the individual complex baseband QAM signal $x_k(t)$ is **sinc-shaped** around the baseband sub-carrier frequency $f_{x,k} = g_k f_\Delta$, with *peak absolute value* $|a_k|T_{obs}$, and it has **zero-crossings** at the frequencies $f = f_{x,k} + if_\Delta$ (for any non-zero integer i). Hence, the width of the **main-lobe** is $2f_\Delta$. *Observe, for future reference, that the signal point a_k is easily found from the value of the Fourier transform in Equation (2.9) evaluated at the baseband sub-carrier frequency $f = f_{x,k} = g_k f_\Delta$ since* $X_{a,k}(f = g_k f_\Delta) = a_k T_{obs}$.

The frequency content in the complex baseband OFDM signal x(t), denoted $X_a(f)$, is now easily found as the sum of the frequency contents of the individual signals $x_k(t)$,

$$X_a(f) = \sum_{k=0}^{K-1} X_{a,k}(f) \tag{2.11}$$

Figure 3b) roughly indicates $X_a(f)$ for an example where $K = 8$.

A short summary of some basic relationships in step 1:

- The definition of f_Δ in Equation (2.1), and also the reason why this definition is chosen.
- The relationship between $x(t)$ and $y(t)$ given by Equations (2.2)-(2.5).
- Observe the close relationship between $Y(f)$ and $X_a(f)$ as is indicated by Figures 3a and 3b (see also Equation (2.7)).
- The Fourier transform $X_a(f)$ of $x(t)$ is given by Equations (2.9)-(2.11) and it is roughly illustrated in Figure 3b.

Step 2: Samples of the complex baseband OFDM signal $x(t)$, and the IDFT.

In connection to Equation (2.5) we emphasized the importance of creating the complex baseband OFDM signal $x(t)$. However, since K is large we do not know how to efficiently create this signal in a straight-forward way in the continuous-time domain. The strategy here is therefore to create $x(t)$ *__indirectly__* by first *__constructing__* time-domain complex samples of $x(t)$. As we will see this strategy will turn out to be successful indeed.

The *__sampling theorem__*, see ref. [1], states that if the highest frequency-component in a signal $s(t)$ is W Hz, then the signal $s(t)$ can be *completely reconstructed* from its samples, if the sampling frequency is at least 2W samples per second.

As mentioned earlier, the K baseband sub-carriers in the complex baseband OFDM signal $x(t)$ are located from $g_0 f_\Delta$ Hz up to $g_{K-1} f_\Delta$ Hz. This means that the **baseband bandwidth** of $x(t)$ is approximately $(g_{K-1} + 1)f_\Delta$ Hz (and the same bandwidth may therefore be assumed also for the real part and for the imaginary part).

Using Equations (1.11) - (1.12), and assuming that $K \gg 1$, **the baseband bandwidth of $x(t)$ is approximately $Kf_\Delta/2$ Hz**. We therefore conclude that the **sampling frequency** f_{samp} should be larger than Kf_Δ samples per second when *__constructing__* the time-domain complex samples of $x(t)$, and large enough such that the sampling theorem can be considered to be sufficiently fulfilled. Note that x(t) is **not** a band-limited signal.

Let us now consider sampling the complex signal $x(t)$ in Equation (2.3) every $\frac{T_{obs}}{N}$ second, i.e. with N samples within the time-interval $0 \le t < T_{obs}$. This corresponds to a sampling frequency f_{samp} equal to,

$$f_{samp} = N/T_{obs} = Nf_\Delta > Kf_\Delta \qquad (2.12)$$

samples per second, and **N should be chosen larger than K**, and large enough such that the sampling theorem can be considered to be sufficiently fulfilled.

Let the column vector (or discrete-time signal) $\boldsymbol{x}$ contain the N time-domain complex samples $x_0, x_1, \dots, x_{N-1}$, of the signal $x(t)$ in Equation (2.3). This means that the sample x_n is,

$$x_n = x(nT_{obs}/N) = \sum_{k=0}^{K-1} a_k e^{j2\pi g_k n/N} \qquad n = 0,1 \dots, (N-1) \qquad (2.13)$$

__Observe that the right hand side of Equation (2.13) actually gives us a way to construct the desired samples $x_0, x_1, \dots, x_{N-1}$ of the complex baseband OFDM signal $x(t)$ (i.e. without actually sample the signal $x(t)$)!__

However, Equation (2.13) does **not** contain the desired size-N IDFT so therefore we need to do some additional work to get another expression for x_n that contains the desired size-N IDFT. Furthermore, we also need an understanding of both the size-N DFT and the size-N IDFT to better understand why and how the former is applied at the receiver side and the latter at the transmitter side.

The **DFT** is closely connected to the Fourier transform $X(v)$ of the discrete-time signal $\boldsymbol{x}$ in Equation (2.13). $X(v)$ is defined by, see ref. [1],

$$X(v) = \sum_{n=0}^{N-1} x_n e^{-j2\pi v n} \tag{2.14}$$

Note in Equation (2.14) that the Fourier transform $X(v)$ is ***periodic in v with period 1***. Furthermore, the variable v can be viewed as a **normalized frequency variable**, $v = f/f_{samp}$. The periodicity in v is illustrated in Figure 4.
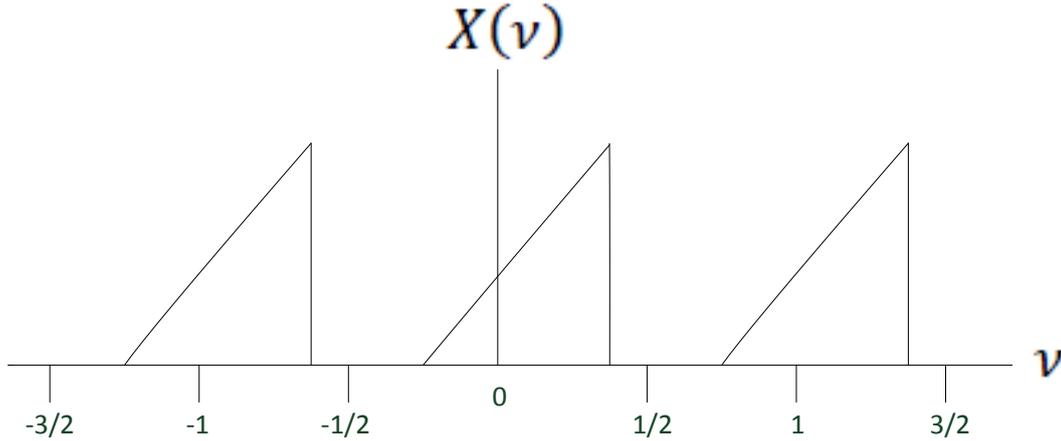
Figure 4. Illustrating that $X(v)$ is periodic in v with period 1. The shape of $X(v)$ in this figure is an example of a Fourier transform of a discrete-time complex signal.

Due to the periodic structure of $X(v)$ it is clear that it is important to understand the behavior of $X(v)$ in the *fundamental interval* $-1/2 \le v \le 1/2$ (corresponding to the frequency interval $-f_{samp}/2 \le f \le f_{samp}/2$).

Furthermore, let X_m denote the **frequency-domain sample** of $X(v)$ at $v = m/N$, defined by

$$X_m = X(v = m/N) = \sum_{n=0}^{N-1} x_n e^{-j2\pi mn/N}, \quad m = 0,1,\dots,N-1 \quad \textbf{(DFT)} \tag{2.15}$$

This is the definition (see ref. [1]) of the size-N **DFT** (Discrete Fourier Transform) of the sequence $\boldsymbol{x}$.

However, for the moment we are particularly interested in the size-N **IDFT** (Inverse Discrete Fourier transform) which is defined by (see ref. [1]),

$$x_n = \frac{1}{N} \sum_{m=0}^{N-1} X_m e^{j2\pi mn/N}, \quad n = 0,1,\dots,N-1 \quad \textbf{(IDFT)} \tag{2.16}$$

Hence, as soon as we have determined the samples in the frequency domain $X_0, X_1, \dots, X_{N-1}$ we should use them in the size-N IDFT in Equation (2.16) to create the desired sequence of time-domain samples $\boldsymbol{x}$! *The values X_m will be determined in step 3.*

In practice, **N is chosen to be a power of 2** since fast Fourier transform (FFT) algorithms then can be used to significantly speed up the calculations in Equations (2.15) - (2.16).

It is clear from the above that the DFT results in frequency-domain samples of $X(v)$. Hence, $X(v)$ is important in the understanding of the DFT. One way to calculate $X(v)$ is to use the definition given in Equation (2.14). Another way to calculate $X(v)$ is to use the fact that the discrete-time signal (or vector) $\boldsymbol{x}$ consists of time-domain samples of the continuous-time (analog) complex baseband OFDM

signal $x(t)$, and there should be a relationship between the frequency contents of these two signals ($X(v)$ and $X_a(f)$, respectively).

The Fourier transform of the signal $x(t)$ is $X_a(f)$ and it is given in Equation (2.11) and also roughly illustrated in Figure 3b.

The relationship between $X(v)$ and $X_a(f)$ can be shown to be (see ref. [1]),

$$X(v) = f_{samp} \sum_{k=-\infty}^{\infty} X_a((v - k)f_{samp}) \tag{2.17}$$

This relationship is very useful indeed, since it gives us complete knowledge about $X(v)$, since $X_a(f)$ is known (from Equations (2.11) and (2.9)). Equation (2.17) tells us that $X(v)$ equals $f_{samp}X_a(vf_{samp})$ **plus** *periodic repetitions* of this function, spaced with normalized frequency 1 apart.

Let us consider an example where $X_a(f)$ is given in Figure 5, and where the baseband bandwidth is denoted W. In Figure 5, $X_a(f) = 0$ outside the frequency range $-2W/3 \leq f \leq W$. Furthermore, assume that the sampling frequency $f_{samp} = \frac{8}{3}W$ samples per second is used. The reader is recommended to apply Equation (2.17) to this example and show that $X(v)$ then will be identical to the Fourier transform given in Figure 4 on the previous page, and the peak value in Figure 4 then equals $f_{samp}B$.
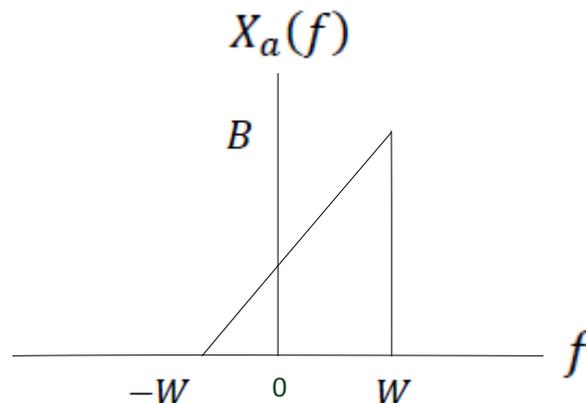
Figure 5. Illustrating $X_a(f)$. The shape of $X_a(f)$ in this figure is an example of a Fourier transform of an analog complex signal (and it does not follow the shape given by Equation (2.11)).

A short summary of some basic relationships in step 2:

- The definition of f_{samp} in Equation (2.12), and also the reason why this definition is chosen.
- The expression of the time-domain samples given in Equation (2.13), and its *derivation*.
- The definition of $X(v)$ in Equation (2.14), and the example given in Figure 4.
- The definition of the size-N DFT in Equation (2.15) and its connection to $X(v)$.
- The definition of the size-N IDFT in Equation (2.16), and its practical consequences at the transmitter side.

Step 3: The relation between the sequences $a_0, a_1, \ldots, a_{K-1}$ and $X_0, X_1, \ldots, X_{N-1}$.

Let us use Equation (2.13) to establish the connection between the sequences $a_0, a_1, \ldots, a_{K-1}$ and $X_0, X_1, \ldots, X_{N-1}$. We rewrite Equation (2.13) in the following way,

$$x_n = x\left(\frac{nT_{obs}}{N}\right) = \sum_{k=0}^{K-1} a_k e^{\frac{j2\pi g_k n}{N}} = \sum_{k=0}^{K-1} a_k e^{j2\pi(g_0+k)n/N} =$$

$$= \sum_{k=0}^{-g_0-1} a_k e^{j2\pi(g_0+k+N)n/N} + \sum_{k=-g_0}^{K-1} a_k e^{j2\pi(g_0+k)n/N} =$$

$$= \sum_{m=g_0+N}^{N-1} a_{m-(g_0+N)} e^{j2\pi mn/N} + \sum_{m=0}^{g_{K-1}} a_{m-g_0} e^{j2\pi mn/N} =$$

$$= \frac{1}{N} \sum_{m=0}^{N-1} X_m e^{j2\pi mn/N} , n = 0,1, \ldots, N-1 \qquad (2.18)$$

Inspection of Equation (2.18) yields the relationships below:

$$X_m = N a_{m-g_0}, \quad \text{if } 0 \le m \le g_{K-1} \qquad (2.19)$$

$$X_m = 0, \quad \text{if } g_{K-1} + 1 \le m \le g_0 + N - 1 \qquad (2.20)$$

$$X_m = N a_{m-(g_0+N)}, \text{if } g_0 + N \le m \le N - 1 \qquad (2.21)$$

The last expression in Equation (2.18) is identical to the size-N IDFT in Equation (2.16). The relation between the sequences $a_0, a_1, \ldots, a_{K-1}$ and $X_0, X_1, \ldots, X_{N-1}$ are given by Equations (2.19) – (2.21).

As an **example:** Consider a situation with K=53 and N=64. In this case $k_{rc} = -g_0 = \frac{K-1}{2} = 26$ and $g_{K-1} = \frac{K-1}{2} = 26$. From Equations (2.19) – (2.21) it is then concluded that the sub-sequence $X_0, X_1, \ldots, X_{26}$ contains the QAM signal points $a_{26}, a_{27}, \ldots, a_{52}$, the sub-sequence $X_{27}, X_{28}, \ldots, X_{37}$ contains only zero values, and the sub-sequence $X_{38}, X_{39}, \ldots, X_{63}$ contains the QAM signal points $a_0, a_1, \ldots, a_{25}$.

As an **example:** Consider the WLAN standard IEEE 802.11n, see the example on page 7. Since K=117 then $k_{rc} = -g_0 = \frac{K-1}{2} = 58$ and $g_{K-1} = \frac{K-1}{2} = 58$. Furthermore, assume that N=128. From Equations (2.19) – (2.21) it is then concluded that the sub-sequence $X_0, X_1, \ldots, X_{58}$ contains the QAM signal points $a_{58}, a_{59}, \ldots, a_{116}$, the sub-sequence $X_{59}, X_{60}, \ldots, X_{69}$ contains only zero values, and the sub-sequence $X_{70}, X_{71}, \ldots, X_{127}$ contains the QAM signal points $a_0, a_1, \ldots, a_{57}$.

As an **example**: Let us consider a situation where K=8 and N=12. In this case $k_{rc} = -g_0 = \frac{K-2}{2} = 3$ and $g_{K-1} = \frac{K}{2} = 4$. From Equations (2.19) – (2.21) it is then concluded that the sub-sequence $X_0, X_1, X_2 X_3, X_4$ contains the QAM signal points a_3, a_4, a_5, a_6, a_7, the sub-sequence X_5, X_6, X_7, X_8 contains only zero values, and the sub-sequence X_9, X_{10}, X_{11} contains the QAM signal points a_0, a_1, a_2.

Even though the relation between the size-K sequence of QAM signal points $a_0, a_1, \ldots, a_{K-1}$ and the size-N sequence of DFT frequency-domain samples $X_0, X_1, \ldots, X_{N-1}$ is already established from Equations (2.18) – (2.21) above it may not be so easy to get an intuitive feeling concerning these results. Therefore additional background material, explanations, result and examples are provided below with the purpose that this material may help the student to increase its understanding and interpretation of the DFT and the IDFT.

Let us therefore take a closer look at the frequency-domain sample $X_l = X(\nu = l/N)$, where l is an arbitrary integer. $X(\nu)$ is roughly indicated in Figure 6 for the example given in Figure 3b where $K = 8$. It is also assumed in Figure 6 that $N = 12$, and this means that $X(\nu)$ is sampled at the normalized frequency $\nu = l/12$ to obtain X_l. The arrows in this figure indicate where the samples X_l are obtained in the normalized frequency domain (i.e. in the ν-domain). ***Observe that the bold indices in Figure 6 indicate the frequency-domain samples that are obtained from the size-12 DFT in Equation (2.15) on page 14***.

Note that the Fourier Transform $X_a(f)$ of $x(t)$ (see Figure 3b) appears frequency-normalized and repeatedly in Figure 6 (compare with Equation (2.17)). This means that the sequence of QAM symbols $a_0, a_1, ..., a_7$ also appears repeatedly in this figure. ***The analog complex baseband QAM signal that carries the QAM symbol a_k is located around the baseband sub-carrier frequency $g_k f_\Delta$ Hz (see Figure 3b and Equation (2.10)), and in Figure 6 the corresponding discrete-time QAM signal appears in the ν-domain around $\nu = \frac{g_k}{N}$ and periodically***.

Since $X(\nu)$ is periodic in ν with period 1, the frequency-domain sample obtained at $\nu = \frac{l}{N}$ will give exactly the same result as the sample obtained at $\nu = \frac{l+N}{N}$. The samples X_l, X_{l-N} and X_{l+N} are therefore identical.

As an **example** in Figure 6: since $K = 8$ and $N = 12$, the QAM symbol a_3 appears at the sampling indices $l = ...$-24,-12,0,12,24,.. (corresponding to $\nu = \cdots, -2, -1, 0, 1, 2, ...$).
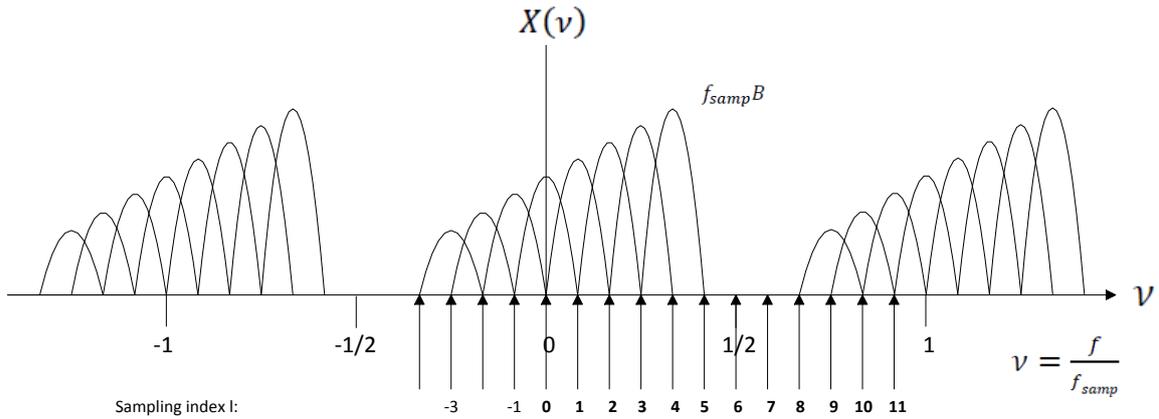
Figure 6. Roughly indicating $X(\nu)$ for the specific example given in Figure 3b where $K = 8$. It is in this figure also assumed that $N = 12$ and the arrows indicate where the frequency-domain samples X_l are obtained. ***The bold indices indicate the frequency-samples that are used by the size-12 IDFT***. Since $K = 8$ and $N = 12$ the QAM symbol a_0 appears at the sampling indices $l = ...$-15,-3,9,21,..

We know that the frequency interval between two successive sub-carrier frequencies is f_Δ Hz. Furthermore, the normalized frequency parameter ν is $\nu = \frac{f}{f_{samp}} = \frac{f}{N f_\Delta}$. This means that in the normalized frequency domain, i.e. in the ν-domain, *the normalized frequency interval between two successive sub-carrier frequencies is* $\frac{f_\Delta}{N f_\Delta} = \frac{1}{N}$.

By definition we also know that the frequency-domain sample X_l is obtained at the normalized frequency $v = l/N$. Hence, the spacing between two successive sampling instants is $1/N$ and, as was discussed above, this is *identical* with the spacing between two successive normalized baseband sub-carrier frequencies. ***This is of fundamental importance since this implies that the l:th sampling instance then occurs at the sub-carrier frequency of a particular normalized baseband QAM frequency spectrum, or at its zero-crossings!*** See Equations (2.9)-(2.11), (2.17), and also Figure 6.

Examples in Figure 6: The frequency-domain sample X_0 is obtained with $l = 0$ and $X_0 = Na_{k_{rc}} = 12a_3$. Hence, t*he frequency-domain sample X_0 will therefore **only** carry information about the QAM symbol $a_{k_{rc}} = a_3$*. It should be noted that the multiplying factor N above can be explained by Equations (2.19)-(2.21), or by taking a closer look at Equations (2.17), (2.11) and (2.9). An alternative explanation is also given below in conjunction with Equation (2.23). Furthermore, the sample $X_{N-k_{rc}} = Na_0$, which in this example means that $X_9 = 12a_0$. Also, the sample $X_{N-1} = Na_{k_{rc}-1}$, which in this example means that $X_{11} = 12a_2$.

Note also in Figure 6, that the baseband sub-carrier frequency $g_7 f_\Delta = 4f_\Delta$ appears at $v = 4/12$. If N would be doubled to N=24 in Figure 6, then this baseband sub-carrier frequency would appear at $v = 4/24$ instead. In general, as N increases with K held fixed, the K normalized baseband sub-carrier frequencies will be more and more concentrated around the integer values of v.

It is fruitful to take a closer look at the impact of the individual signal $x_k(t)$ on the frequency-domain sample X_l. Therefore, consider the Fourier transform of the discrete-time signal obtained if **only** time-domain samples from $x_k(t)$ are considered, i.e. the Fourier transform of the discrete-time signal,

$$a_k e^{j2\pi g_k n/N}, \qquad n = 0, 1, ..., (N-1) \tag{2.22}$$

The Fourier transform of the discrete-time signal in Equation (2.22) can be expressed as,

$$\sum_{n=0}^{N-1} a_k e^{j2\pi g_k n/N} e^{-j2\pi vn} = a_k \frac{\sin(\pi N(v - g_k/N))}{\sin(\pi(v - g_k/N))} e^{-j\pi(v - g_k/N)(N-1)} \tag{2.23}$$

To get the result in Equation (2.23) we have identified a geometric series in the left-hand side. By investigating Equation (2.23) for $v = \frac{g_k}{N}$ we find that the value equals $a_k N$. Also, by investigating Equation (2.23) for $v = \frac{g_k + J}{N}$, where $J = 1, 2, ..., (N-1)$, we find that the value equals zero.

Hence, the value of Equation (2.23) is $a_k N$ if $v = \frac{g_k}{N} + i$, where i denotes an arbitrary integer (periodicity).

As a consequence of the above we conclude that if the Fourier transform in Equation (2.23) is sampled at the normalized frequency $v = l/N$, then a **non-zero** result is obtained **only** if $l = g_k + iN$, where i denotes an arbitrary integer, and the non-zero result equals the value $a_k N$.

Therefore, if the specific frequency-domain sample X_l is non-zero then only **<u>one</u>** of the K QAM signals will contribute to the value of X_l,

$$X_l = a_k N \tag{2.24}$$

and the particular value of k is defined by,

$$g_k = l - iN \tag{2.25}$$

This means that we now can determine the N frequency-domain samples X_l, $l = 0, 1, ..., (N-1)$ that are obtained from the size-N DFT in Equation (2.15) on page 14.

For $0 \le l \le g_{K-1}$ we find from Equation (2.25) that $g_k = l$, and the corresponding value of k is known from Equations (1.8)-(1.9). Therefore,

$$k = k_{rc} + g_k = k_{rc} + l \tag{2.26}$$

$$X_l = N a_{k_{rc}+l} \qquad l = 0, 1 \ldots, g_{K-1} \tag{2.27}$$

Observe that Equation (2.27) is equivalent with Equation (2.19).

For $g_0 + N \le l \le (N-1)$ we find from Equation (2.25) that $g_k = l - N$, and the corresponding values of k and X_l are ($g_0 = -k_{rc}$),

$$k = k_{rc} + g_k = k_{rc} + l - N \tag{2.28}$$

$$X_{-k_{rc}+N+k} = N a_k \qquad k = 0, 1, \ldots (k_{rc} - 1) \tag{2.29}$$

Observe that Equation (2.29) is equivalent with Equation (2.21).

For the <u>*intermediate interval*</u> $(g_{K-1} + 1) \le l \le (g_0 + N - 1)$, that covers the remaining (N-K) frequency-domain samples, the values of these samples are $X_l = 0$. Compare with Figure 6 on page 17 where $(N - K) = 4$ and where $X_5 = X_6 = X_7 = X_8 = 0$.

It should be noted that the results on X_l above are identical with the results obtained in Equations (2.19) – (2.21).

Observe from Equations (2.27) and (2.29) that the desired sequence $X_0, X_1, ..., X_{N-1}$ is very easy to construct by using the K signal-points, and $(N - K)$ zeroes! This is shown below.

If we first construct the size-N sequence $N a_0, N a_1, .., N a_{K-1}, 0, 0, .., 0$, and then "left-rotate" this sequence k_{rc} positions (or "right-rotate" this sequence $(g_0 + N)$ positions), then the desired sequence $X_0, X_1, ..., X_{N-1}$ in Equations (2.27) and (2.29) is obtained!

Consider as an **example** the case K=8 and N=12. In this case $k_{rc} = 3$ and $g_{K-1} = 4$, and the desired sequence $X_0, X_1, ..., X_{11}$ then equals: $N a_3, N a_4, N a_5, N a_6, N a_7, 0, 0, 0, 0, N a_0, N a_1, N a_2$. See also Figure 6.

The final step is to calculate the size-N **IDFT**,

$$x_n = \frac{1}{N}\sum_{m=0}^{N-1} X_m e^{j2\pi mn/N}, \qquad n = 0, 1, \ldots, N-1 \qquad (2.30)$$

In practice, **N is chosen to be a power of 2** since fast Fourier transform (FFT) algorithms can then be used to significantly speed up the calculations in equation (2.30).

Equation (2.30) is the desired final expression to compute the discrete-time signal x, i.e. the N time-domain samples of the complex baseband OFDM signal $x(t)$. Equation (2.30), i.e. the size-N IDFT, is computationally very efficient when implemented using FFT algorithms (if N is chosen to be a power of 2). The sequence $X_0, X_1, \ldots, X_{N-1}$ is given by Equations (2.27) and (2.29) or alternatively by Equations (2.19)-(2.21). See also the construction ("rotation") given above. See also Figure 7 on page 27.

The $(N - K)$ zeroes in the sequence $X_0, X_1, \ldots, X_{N-1}$ may be interpreted as using zero-valued signal-points at baseband sub-carrier frequencies located at the edges but outside of the OFDM frequency band.

As an example of an application let us consider LTE-systems (Long-Term Evolution). In LTE (from ref. [9]), OFDM is used and $f_\Delta = \frac{1}{T_{obs}} = 15$ kHz which means that $T_{obs} = 66.67$ µs. Furthermore, assume that, e.g., K=720 sub-carriers are used and that N=1024 is chosen. The OFDM bandwidth is then approximately $Kf_\Delta = 10.8$ MHz around the carrier frequency, and the chosen sampling frequency is $f_{samp} = Nf_\Delta = 15.36$ Msample per second. A typical OFDM interval in LTE is 71.36 µs, and 14 OFDM signals (i.e. 14 size-1024 IDFT calculations) are then generated every ms.

It is clear from the numbers in the example above that very fast and computationally efficient implementations are required to be able to build the state-of-the-art communication systems of today. It is recommended that the reader reflects over the implementation parameters given in the example above, including the size of the unit and its power-consumption (and cooling requirements).

It should also be mentioned here that the "rotation" operation described on the previous page can alternatively be expressed as a **matrix multiplication**. Define the size-K column vector $\boldsymbol{a}$ by $\boldsymbol{a}^{tr} = (a_0\ a_1\ \ldots\ a_{K-1})$, where "tr" denotes transpose. Furthermore, define the size-N column vector $\boldsymbol{X}$ by $\boldsymbol{X}^{tr} = (X_0\ X_1\ \ldots X_{N-1})$.

Then, by examining Equations (2.27) and (2.29), the "rotation" operation can be described by the following expression,

$$\boldsymbol{X} = N\boldsymbol{Q}_t\boldsymbol{a} \qquad (2.31)$$

where the size NxK matrix $\boldsymbol{Q}_t$ has the value one in the (i,j):th elements given below (the rows are numbered from 0 to (N-1), and the columns are numbered from 0 to (K-1) :

$$(i,j): (0, k_{rc}), (1, k_{rc} + 1), (2, k_{rc} + 2), \ldots, (g_{K-1}, K - 1) \qquad (2.32)$$

$$(i,j): (N - k_{rc}, 0), (N - k_{rc} + 1, 1), (N - k_{rc} + 2, 2), \ldots, (N - 1, k_{rc} - 1) \qquad (2.33)$$

The total number of matrix element positions given in Equations (2.32)-(2.33) is K, and the value of each corresponding matrix element is one. For the remaining matrix elements in $\boldsymbol{Q}_t$ the value is zero.

Note that the operation in Equation (2.31) automatically places N-K zeroes in the sequence X since the matrix Q_t has N-K rows that contain only zeroes. Furthermore, every column in the matrix Q_t has only one element that is equal to one. See the two examples below.

Example: If K=8 and N=12 in Equations (2.32)-(2.33), then Q_t equals ($k_{rc} = 3$ and $g_7 = 4$) :

$$Q_t = \begin{pmatrix} 0 & 0 & 0 & 1 & 0 & 0 & 0 & 0 \\ 0 & 0 & 0 & 0 & 1 & 0 & 0 & 0 \\ 0 & 0 & 0 & 0 & 0 & 1 & 0 & 0 \\ 0 & 0 & 0 & 0 & 0 & 0 & 1 & 0 \\ 0 & 0 & 0 & 0 & 0 & 0 & 0 & 1 \\ 0 & 0 & 0 & 0 & 0 & 0 & 0 & 0 \\ 0 & 0 & 0 & 0 & 0 & 0 & 0 & 0 \\ 0 & 0 & 0 & 0 & 0 & 0 & 0 & 0 \\ 0 & 0 & 0 & 0 & 0 & 0 & 0 & 0 \\ 1 & 0 & 0 & 0 & 0 & 0 & 0 & 0 \\ 0 & 1 & 0 & 0 & 0 & 0 & 0 & 0 \\ 0 & 0 & 1 & 0 & 0 & 0 & 0 & 0 \end{pmatrix}$$

Example: If K=9 and N=12 in Equations (2.32)-(2.33), then Q_t equals ($k_{rc} = 4$ and $g_8 = 4$) :

$$Q_t = \begin{pmatrix} 0 & 0 & 0 & 0 & 1 & 0 & 0 & 0 & 0 \\ 0 & 0 & 0 & 0 & 0 & 1 & 0 & 0 & 0 \\ 0 & 0 & 0 & 0 & 0 & 0 & 1 & 0 & 0 \\ 0 & 0 & 0 & 0 & 0 & 0 & 0 & 1 & 0 \\ 0 & 0 & 0 & 0 & 0 & 0 & 0 & 0 & 1 \\ 0 & 0 & 0 & 0 & 0 & 0 & 0 & 0 & 0 \\ 0 & 0 & 0 & 0 & 0 & 0 & 0 & 0 & 0 \\ 0 & 0 & 0 & 0 & 0 & 0 & 0 & 0 & 0 \\ 1 & 0 & 0 & 0 & 0 & 0 & 0 & 0 & 0 \\ 0 & 1 & 0 & 0 & 0 & 0 & 0 & 0 & 0 \\ 0 & 0 & 1 & 0 & 0 & 0 & 0 & 0 & 0 \\ 0 & 0 & 0 & 1 & 0 & 0 & 0 & 0 & 0 \end{pmatrix}$$

For future reference let us also observe that the vector a can be recovered from the vector X by a "re-rotation",

$$a = \frac{1}{N} Q_r X \tag{2.34}$$

where the size KxN matrix Q_r is defined by,

$$Q_r = Q_t^{tr} \tag{2.35}$$

Furthermore, the size KxK matrix $Q_r Q_t$ is the identity matrix, while the size NxN matrix $Q_t Q_r$ has K ones and N-K zeroes on the main diagonal (and the remaining elements are zero).

Let us now introduce a compact and convenient description of the DFT and IDFT operations that is based on matrices. Therefore, consider the (symmetric) size NxN matrix $\boldsymbol{F}$ with matrix elements $F_{k,n}$,

$$F_{m,n} = e^{-j2\pi mn/N} \tag{2.36}$$

The sequence (column vector) of frequency-domain samples $\boldsymbol{X}$ obtained from the DFT operation in Equation (2.15) can then be written as,

$$\boldsymbol{X} = \boldsymbol{F}\boldsymbol{x} \qquad \textbf{(DFT)} \tag{2.37}$$

and the column vector $\boldsymbol{x}$ contains the N time-domain complex samples $x_0, x_1, \dots, x_{N-1}$, of the signal $x(t)$ in Equation (2.3).

In the same way consider the (symmetric) size NxN matrix $\boldsymbol{G}$ with matrix elements $G_{m,n}$,

$$G_{m,n} = e^{j2\pi mn/N} \tag{2.38}$$

The sequence of time-domain samples $\boldsymbol{x}$ obtained from the IDFT operation in Equation (2.16) can then be written as,

$$\boldsymbol{x} = \frac{1}{N}\boldsymbol{G}\boldsymbol{X} \qquad \textbf{(IDFT)} \tag{2.39}$$

By combining Equation (2.31) and Equation (2.39) we obtain the compact description,

$$\boldsymbol{x} = \frac{1}{N}\boldsymbol{G}N\boldsymbol{Q}_t\boldsymbol{a} \tag{2.40}$$

The matrices $\boldsymbol{F}$ and $\boldsymbol{G}$ are such that the size NxN matrix $\frac{1}{N}\boldsymbol{F}\boldsymbol{G}$ is the identity matrix. Furthermore, for future reference (in section 6), by combining Equation (2.34), Equation (2.37) and Equation (2.40) we obtain the equalities,

$$\boldsymbol{a} = \frac{1}{N}\boldsymbol{Q}_r\boldsymbol{X} = \frac{1}{N}\boldsymbol{Q}_r\boldsymbol{F}\boldsymbol{x} = \frac{1}{N}\boldsymbol{Q}_r\boldsymbol{F}\frac{1}{N}\boldsymbol{G}N\boldsymbol{Q}_t\boldsymbol{a} \tag{2.41}$$

An **alternative** way to determine the impact of the individual signal $x_n(t)$ on X_l is to first use Equation (2.17) to determine the Fourier transform of the discrete-time signal in Equation (2.22). The second step is then to sample this Fourier transform at $\nu = l/N$ and investigate its value.

We have already found the Fourier transform of the analog signal $x_n(t)$, see Equation (2.9), and it was found that its spectrum is **sinc-shaped** around the baseband sub-carrier frequency $g_k f_\Delta$ Hz , with *peak absolute value* $|a_k|T_{obs}$, and with **zero-crossings** at the frequencies $f = g_k f_\Delta + i f_\Delta$ (for any non-zero integer i). Hence, the width of the **main-lobe** is $2f_\Delta$ Hz.

From Equation (2.17) it is also known how to obtain the Fourier transform of the discrete-time signal if the Fourier transform of the corresponding analog signal is known.

Therefore, the Fourier transform of the discrete-time signal in Equation (2.22) equals,

$$f_{samp}X_{a,k}\left(\nu f_{samp}\right) = f_{samp}a_k T_{obs} \frac{sin\left(\pi\left(\nu f_{samp}-\frac{g_k}{T_{obs}}\right)T_{obs}\right)}{\pi\left(\nu f_{samp}-\frac{g_k}{T_{obs}}\right)T_{obs}} e^{-j\pi\left(\nu f_{samp}-\frac{g_k}{T_{obs}}\right)T_{obs}} \tag{2.42}$$

plus *periodic repetitions of this function*, spaced with normalized frequency 1 apart.

Let us now use that $f_{samp} = N/T_{obs}$. Then Equation (2.42) is simplified to,

$$f_{samp}X_{a,k}\left(\nu f_{samp}\right) = N a_k \frac{sin(\pi N(\nu-g_k/N))}{\pi N(\nu-g_k/N)} e^{-j\pi N(\nu-g_k/N)} \tag{2.43}$$

An important observation now is that sampling the frequency-function in equation (2.43), at the normalized frequency $\nu = l/N$, results in a **non-zero** value **only** if $l = g_k$, and this non-zero value equals $a_k N$.

So, the impact on X_l from the individual signal $x_n(t)$ is therefore found to be equal to $a_k N$ **only** for the indices $l = g_k + iN$, where i denotes an arbitrary integer (due to the periodicity in ν with period 1), and zero for any other l. *Observe that this is exactly the _same result_ as was obtained earlier in connection to Equation (2.24) following an alternative path.*

It is instructive to compare Equation (2.43) with Equation (2.23), especially in the fundamental interval $-1/2 \leq \nu \leq 1/2$. The reason why these two expressions are different is that the Fourier transform in equation (2.23) includes the total effect of _aliasing_ (aliasing is a consequence when the chosen sampling frequency does not satisfy the sampling theorem, and the effect of aliasing therefore decreases as N increases), while equation (2.43) only represents the contribution to the Fourier transform given by the term corresponding to the index k=0 in Equation (2.17).

In the next section we will add (append) the so-called cyclic prefix (CP) to the vector $\boldsymbol{x}$ of time-domain samples (see Equation (2.30)), and also use digital-to-analog (D/A) converters to create the analog real signals that are needed in the construction of the desired OFDM signal.

A short summary of some basic relationships in step 3:

- The size-N input sequence to the IDFT, i.e. the frequency-domain samples obtained from the DFT, are obtained from Equations (2.18) - (2.21) (note that N-K samples are equal to zero).
- The examples on page 16 are strongly recommended.
- Figure 6 on page 17 illustrates $X(\nu)$ for a specific case, and this figure also indicates where the QAM symbols are located along the normalized frequency axis. ***Observe that the bold indices in this figure indicate those frequency-domain samples that are used by the size-12 IDFT.***
- The **Examples in Figure 6** on page 18 are strongly recommended.
- The size-N input sequence to the IDFT, i.e. the frequency-domain samples obtained from the DFT, are also given by Equations (2.27) and (2.29) (the remaining N-K samples are equal to zero). Observe the "rotation" construction on page 19!
- Observe the practical importance of Equation (2.30). See also Figure 7 on page 27.
- Compact matrix descriptions are found on pages 20-22.

Section 3: The Cyclic Prefix (CP) and Digital-to-Analog (D/A) conversion

Adding (appending) the Cyclic prefix (CP)

In the previous section we found how the size-N IDFT could be used to efficiently create N time-domain complex samples of the equivalent complex baseband OFDM signal $x(t)$ in Equations (2.2) and (2.3). These N samples will in this section be time-shifted T_{CP} seconds and they then become the time-domain samples of the OFDM signal $x(t - T_{CP})$ within the time-interval $T_{CP} \leq t \leq T_s$, i.e. within the observation interval of the receiver. We will in this section also specify the remaining L time-domain samples of the OFDM signal that correspond to the cyclic prefix (CP) within the time-interval $0 \leq t \leq T_{CP}$.

The OFDM signal that we are in progress to synthesize has a CP of duration T_{CP} in the beginning of the OFDM signal interval T_s, and the remaining part of the OFDM signal has duration $T_{obs}=T_s - T_{CP}$. As was mentioned in the first section, the main purpose of the CP is to allow for the initial transient behavior of the multi-path channel _output_ signal to occur within the duration of the CP. In a sense, the CP acts as a "guard interval" in the time-domain.

It is also very important that the duration of the cyclic prefix is at least as large as the duration of the impulse response of the channel. This will be explained in detail in section 5. An additional requirement is that $T_{CP} \ll T_s$.

As an **example**: In LTE (from [9]) a typical choice of T_{CP} is $T_{CP} = 4.69$ µs which is 6.57 % of the OFDM symbol interval T_s.

In this section **we will construct the CP by adding (appending) L additional time-domain samples before the already created N samples**. As will be seen, the CP is constructed by adding a so-called size-L _periodic extension_ of the N samples. In this way all $L + N$ samples of a complex baseband OFDM signal within the time-interval $0 \leq t \leq T_s$ is obtained, and $T_{CP} = LT_{obs}/N$. The remaining steps is then D/A converters (also in this section) and frequency up-conversion (in section 4).

Now observe that the signal $x(t)$ in Equation (2.3) has duration T_{obs}. However, the expression that is used to define $x(t)$ equals $\sum_{k=0}^{K-1} a_k e^{j2\pi g_k f_\Delta t}$, and this expression is **periodic in t with period T_{obs}**. Therefore, this expression is _identical_ within the two time-intervals $-T_{CP} \leq t \leq 0$ and $(T_{obs} - T_{CP}) \leq t \leq T_{obs}$. _Observe now that the waveform corresponding to the first time-interval_ $-T_{CP} \leq t \leq 0$ _is used to define the so-called_ **cyclic prefix** (CP). Furthermore, L samples of this waveform that defines the CP will be _identical_ to the L last samples in the size-N vector **x**, since the L last samples in **x** are samples that correspond to the latter time-interval $(T_{obs} - T_{CP}) \leq t \leq T_{obs}$.

So, if we consider the expression $\sum_{k=0}^{K-1} a_k e^{j2\pi g_k f_\Delta t}$ _only_ within the time-interval $-T_{CP} \leq t \leq T_{obs}$ it defines an OFDM signal, and the OFDM signal interval is $T_s = T_{CP} + T_{obs}$. Furthermore, all L+N time-domain samples are known since the size-N vector **x** has already been created, and, as was described above, the L samples corresponding to the CP are identical to the last L samples in **x**.

Since we should have a _**causal**_ OFDM signal we need to introduce a time-delayed version of the expression studied above. With a time delay equal to T_{CP} seconds we get the expression $\sum_{k=0}^{K-1} a_k e^{j2\pi g_k f_\Delta (t-T_{CP})}$ within the OFDM signal interval $0 \leq t \leq T_S$. _**This is the final desired expression for the synthesized complex baseband OFDM signal.**_

What remains to be done in the digital domain is to construct a new size-(L+N) vector $\boldsymbol{u}$ that contains all (L+N) time-domain samples of the expression $\sum_{k=0}^{K-1} a_k e^{j2\pi g_k f_\Delta (t-T_{CP})}$ within the OFDM signal interval $0 \le t \le T_S$.

Based on the discussion about periodicity above let us therefore construct a new size-(L+N) vector $\boldsymbol{u}$ as a so-called _periodic extension_ of the size-N vector $\mathbf{x}$. This means that *the L last samples in $\boldsymbol{x}$ are copied and placed as the first L samples in $\boldsymbol{u}$*. The remaining N samples in $\boldsymbol{u}$ are identical to $\boldsymbol{x}$. This means that,

$$u_0 = x_{N-L}, \ldots, u_{L-1} = x_{N-1}, u_L = x_0, \ldots, u_{L+N-1} = x_{N-1}. \tag{3.1}$$

The construction of the vector $\boldsymbol{u}$ above implies that the first L samples in $\boldsymbol{u}$ are identical with the last L samples in $\boldsymbol{u}$, and this reflects the periodicity discussed above.

The duration of the OFDM signal interval is T_s, and it can be expressed as,

$$T_S = \frac{(L+N)T_{obs}}{N} = T_{CP} + T_{obs} \tag{3.2}$$

The vector $\boldsymbol{u}$ in equation (3.1) contains (L+N) time-domain complex samples of a complex baseband OFDM signal defined over the entire OFDM signal interval $0 \le t \le T_S$. This complex baseband OFDM signal is here denoted $\boldsymbol{u(t)}$, and based on the previous discussion in this section, the OFDM signal $\boldsymbol{u(t)}$ is,

$$u(t) = u_{Re}(t) + ju_{Im}(t) = \sum_{k=0}^{K-1} a_k e^{j2\pi g_k f_\Delta (t-T_{CP})}, \quad 0 \le t \le T_S \tag{3.3}$$

and $u(t)$ equals zero outside this interval. The OFDM signal $u(t)$ in Equation (3.3) includes the CP of duration T_{CP} and also the observation interval of duration T_{obs}. Furthermore, the m:th sample in the vector $\boldsymbol{u}$ is,

$$u_m = u(mT_{obs}/N), \quad m = 0,1, \ldots, (L+N-1) \tag{3.4}$$

As we will see in section 4, and in analogy with Equations (2.2) and (2.5), the desired real high-frequency OFDM signal, here denoted $s(t)$, is obtained as,

$$s(t) = Re\{u(t)e^{j2\pi f_{rc}t}\} = u_{Re}(t)\cos(2\pi f_{rc}t) - u_{Im}(t)\sin(2\pi f_{rc}t) \tag{3.5}$$

Our work in the discrete-time (digital) domain is now finished and it is time to enter the continuous-time (analog) domain. The practical way to do this is to use D/A converters.

D/A conversion

In analogy with Equation (3.5) the construction of the desired real high-frequency OFDM signal $s(t)$ is straight-forward ($s_I(t) = u_{Re}(t)$, and $s_Q(t) = u_{Im}(t)$),

$$s(t) = s_I(t)\cos(2\pi f_{rc}t) - s_Q(t)\sin(2\pi f_{rc}t) \tag{3.6}$$

Hence, we first need to construct the two analog signals $s_I(t)$ and $s_Q(t)$ that correspond to the real part $\boldsymbol{u}_{Re}$ and to the imaginary part $\boldsymbol{u}_{Im}$ of the vector $\boldsymbol{u}$ in Equations (3.1) and (3.4), respectively, where

$$\boldsymbol{u} = \boldsymbol{u}_{Re} + j\boldsymbol{u}_{Im} \tag{3.7}$$

These two real-valued sequences each feeds a separate D/A converter as is illustrated in Figure 7, and the samples in each sequence arrive with the rate $f_{samp} = Nf_\Delta$ samples per second.
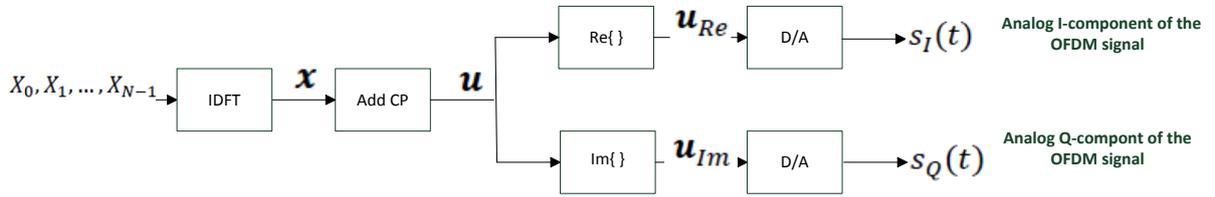
Figure 7. Block diagram illustrating the operations in the digital domain, and the transition to the analog domain. The IDFT is given in Equation (2.30) (and in Equation (2.18)).

Let $s_I(t)$ denote the analog output signal (i.e. the I-component of the OFDM signal) that results from the sequence (or vector) $\boldsymbol{u}_{Re}$. In the same way, let $s_Q(t)$ denote the analog output signal (i.e. the Q-component of the OFDM signal) that results from the sequence (or vector) $\boldsymbol{u}_{Im}$.

We will now go through the D/A conversion of the discrete-time signal $\boldsymbol{u}_{Re}$ to the continuous-time (analog) signal $s_I(t)$.

The ideal goal of the D/A converter is to create as output signal an continuous-time (analog) voltage waveform that preserves the samples in $\boldsymbol{u}_{Re}$ in the time-domain, and **also** preserves the frequency content of $\boldsymbol{u}_{Re}$ within the fundamental interval $-f_{samp}/2 \leq f \leq f_{samp}/2$, i.e. within the normalized interval $-1/2 \leq \nu \leq 1/2$ (compare with Figure 6 on page 17, but assume now a spectrum that is symmetric around $\nu = 0$, since $\boldsymbol{u}_{Re}$ is a *real* sequence). Ideally, given the samples in $\boldsymbol{u}_{Re}$, and given the sampling frequency f_{samp}, the output analog waveform can be determined and it is *unique*.

The overall operation of the D/A converter may be interpreted as an *interpolation*, and typically this can be achieved by constructing the signal $s_I(t)$ as,

$$s_I(t) = \sum_{m=0}^{L+N-1} u_{Re,m}\, g_i\left(t - \frac{mT_{obs}}{N}\right) \tag{3.8}$$

where $g_i(t)$ is referred to as an *interpolation filter* or *reconstruction filter*. Note in Equation (3.8) that $s_I(t)$ is created by multiplying the m:th sample $u_{Re,m}$ with a time-dependent and m-dependent function $g_i\left(t - \frac{mT_{obs}}{N}\right)$, and then all L+N such contributions are added.

Hence, in general the value $s_I(t)$ is created using all elements in the vector $\boldsymbol{u}_{Re}$. However, as is also seen in Equation (3.8), the total contribution to the output $s_I(t)$ from the individual sample $u_{Re,m}$ equals,

$$u_{Re,m} g_i\left(t - \frac{mT_{obs}}{N}\right) \tag{3.9}$$

and Equation (3.8) is the superposition of L+N such contributions.

Furthermore, at the m:th sampling-time we know that $s_I\left(\frac{mT_{obs}}{N}\right) = u_{Re,m}$ which means that $g_i(t = 0) = 1$, and $g_i\left(t = \frac{lT_{obs}}{N}\right) = 0$ where l is any non-zero integer.

It is therefore reasonable to assume that the contribution in Equation (3.9) is large at, and around, $t = \frac{mT_{obs}}{N}$ and then gets "smaller" as t moves away from this value. In summary; the filter $g_i(t)$ should have its peak value 1 at $t = 0$, should be equal to zero at $t = \frac{lT_{obs}}{N}$ where l is any non-zero integer, and in general "decay" as $|t|$ increases.

Let $U_{Re}(\nu)$ denote the Fourier transform of the discrete-time signal $\boldsymbol{u}_{Re}$, and let $S_I(f)$ denote the Fourier transform of the output continuous-time signal $s_I(t)$. An important observation is that Equation (3.8) can be interpreted as an **analog filtering operation**, where $g_i(t)$ is the impulse response of the filter and $G_i(f)$ denotes the transfer function of the filter.

The analog input signal to the filter may be expressed as $\sum_{m=0}^{L+N-1} u_{Re,m} \delta\left(t - \frac{mT_{obs}}{N}\right)$. It is left as an exercise to the reader to show that, with $f_{samp} = Nf_\Delta$,

$$S_I(f) = U_{Re}(\nu = f/f_{samp})G_i(f) \tag{3.10}$$

Note that since $U_{Re}(\nu)$ is periodic in ν with period 1, the Fourier transform $U_{Re}(\nu = f/f_{samp})$ of the analog input signal **is periodic in f with period f_{samp}.**

Hence, to extract *only* the desired frequency content in $\boldsymbol{u}_{Re}$ corresponding to the fundamental frequency interval $-f_{samp}/2 \leq f \leq f_{samp}/2$ **the transfer function $G_i(f)$ of the filter should have low-pass characteristics** with an ideal cut-off frequency equal to $f_{samp}/2$ Hz.

It is here instructive to investigate some properties of the **ideal** reconstruction filter. This filter can be derived from the sampling theorem and the result is a filter with infinite duration, see ref. [1],

$$g_{i,ideal}(t) = \frac{\sin(\pi f_{samp} t)}{\pi f_{samp} t} \tag{3.11}$$

If this ideal filter is used in Equation (3.8) then we find that the particular sample $s_I(t = kT_{obs}/N) = s_I(t = k/f_{samp}) = u_{Re,k}$, and this is due to the zero-crossings in $g_{i,ideal}(t)$.

Furthermore, this ideal filter is actually an ideal low-pass filter i.e. having a non-zero (and symmetric) transfer function **only** within the frequency interval $-f_{samp}/2 \leq f \leq f_{samp}/2$,

$$G_{i,ideal}(f) = 1/f_{samp}, \quad -f_{samp}/2 \leq f \leq f_{samp}/2 \tag{3.12}$$

Hence, using this ideal filter in Equation (3.8) indeed extracts only the fundamental frequency interval.

However, there are some practical difficulties with the ideal filter such as its non-causal property and the infinite duration of its impulse response.

Instead of trying to implement a single filter $g_i(t)$ with sufficiently good properties, it is common to split $g_i(t)$ into two filters denoted $g_{i,1}(t)$ and $g_{i,2}(t)$. First the simpler filter $g_{i,1}(t)$ is used in Equation (3.8). The resulting analog signal from this filter is then filtered with the second filter $g_{i,2}(t)$. The final output signal from the second filter then has the Fourier transform,

$$U_{Re}(v = f/f_{samp})G_{i,1}(f)G_{i,2}(f) = U_{Re}(v = f/f_{samp})G_i(f) \tag{3.13}$$

Hence, the convolution between $g_{i,1}(t)$ and $g_{i,2}(t)$ equals the overall filter $g_i(t)$.

A typical choice of the first filter is $g_{i,1}(t) = 1$ in the time-interval $0 \leq t \leq T_{obs}/N$, and $g_{i,1}(t) = 0$ outside this interval. The analog output signal from this filter is then a so-called **staircase**-function, i.e. the output signal consists of a sequence of T_{obs}/N-long rectangular pulses where the amplitude of the m:th pulse equals the value of the sample $u_{Re,m}$. Therefore, this choice of filter is referred to as S/H filter (**Sample-and-Hold**).

The Fourier transform of the S/H filter $g_{i,1}(t)$ above is,

$$G_{i,1}(f) = \frac{1}{f_{samp}} \frac{sin(\pi f/f_{samp})}{\pi f/f_{samp}} e^{-j\pi f/f_{samp}} \tag{3.14}$$

which is significantly different then $G_{i,ideal}(f)$ in Equation (3.12).

To improve the D/A conversion above let us, as an example, choose the second filter as $g_{i,2}(t) = f_{samp}g_{i,1}(t)$ where $G_{i,1}(f)$ is given by Equation (3.14). The overall filter $g_i(t)$ is then **triangular**, with peak value equal to 1 at $t = T_{obs}/N$ and with duration $2T_{obs}/N$ (symmetric around $t = T_{obs}/N$). *Observe* that the analog output signal from this second filter then consists of **straight lines connecting the sample values**. *Observe also* that a **time-delay** equal to T_{obs}/N (corresponding to a sampling interval) here is obtained.

The Fourier transform of the overall triangular filter $g_i(t)$ is,

$$G_i(f) = \frac{1}{f_{samp}} \left(\frac{sin\left(\frac{\pi f}{f_{samp}}\right)}{\frac{\pi f}{f_{samp}}}\right)^2 e^{-j2\pi f/f_{samp}} \tag{3.15}$$

and with this filter a more efficient overall low-pass filtering is obtained. Furthermore, the phase function is a linear function of frequency over the fundamental frequency interval of interest, and it is seen in the exponential in Equation (3.15) that the linear phase corresponds to the time-delay T_{obs}/N ($=1/f_{samp}$).

In case additional improvements in the D/A conversion process are needed additional low-pass filtering can be implemented. One possibility may be to try to synthesize an overall interpolation filter that is a symmetrically time-truncated and time-delayed version of the ideal filter. There is also the possibility of digital filtering of the sequence $\mathbf{u}_{Re}$ before D/A-conversion, which may relax the requirements on the analog interpolation filter. It should however be observed that efficient high precision (e.g. 16 bits per sample or more) D/A and A/D converters operating at high sampling frequencies are challenging to implement in practice, and different implementation strategies may be used.

This concludes our introductory treatment on D/A-converters. To simplify the presentations in the next sections we will here assume that the two signals $s_I(t)$ and $s_Q(t)$ are almost perfectly reconstructed using almost ideal D/A-converters in Figure 7 on page 27. This means that we will assume throughout that both $S_I(f)$ and $S_Q(f)$ can be closely approximated to be ideal. Hence, it is assumed that both these frequency functions are equal to zero outside the frequency interval $-f_{samp}/2 \leq f \leq f_{samp}/2$, and within this interval they are equal to,

$$S_I(f) = \frac{1}{f_{samp}} U_{Re}\left(\nu = \frac{f}{f_{samp}}\right), \quad in \quad -f_{samp}/2 \leq f \leq f_{samp}/2 \tag{3.16}$$

$$S_Q(f) = \frac{1}{f_{samp}} U_{Im}\left(\nu = \frac{f}{f_{samp}}\right), \quad in \quad -f_{samp}/2 \leq f \leq f_{samp}/2 \tag{3.17}$$

In the time domain Equations (3.16)-(3.17) mean that we assume that (from Equation (3.3)),

$$s_I(t) + js_Q(t) = \sum_{k=0}^{K-1} a_k e^{j2\pi g_k f_\Delta (t - T_{CP})}, \quad 0 \leq t \leq T_s \tag{3.18}$$

We are now ready for the final stages in the transmitter, i.e. frequency up-conversion, power amplification and the antenna coupling unit.

A short summary of some basic relationships in Section 3:

- Equation (3.1) specifies the size-(L+N) vector of time-domain samples that represents the entire OFDM signal interval. See also Equation (3.4).
- Observe that the first L samples in $\boldsymbol{u}$ are identical with the last L samples in $\boldsymbol{u}$.
- The cyclic prefix is represented by the first L samples in the vector $\boldsymbol{u}$, see also Equation (3.2).
- Observe the importance of Equations (3.3) and (3.5).
- Figure 7 on page 27 illustrates the operations in the digital domain, and the transition to the analog domain.
- Observe the interpretation of the D/A conversion process as an analog filter operation.
- The consequences of D/A conversion using a "sample-and-hold" reconstruction filter or a "triangular" reconstruction filter, respectively, are discussed on page 29.
- Observe in Equations (3.16)-(3.18) and in Figure 7 that (ideally) the continuous-time I and Q signals of the desired OFDM signal are obtained after the D/A units.

Section 4: Frequency up-conversion and power amplification

Similar to Equation (3.6) the construction of the OFDM signal $s(t)$ is straight-forward,

$$s(t) = s_I(t)\cos(2\pi f_{rc}t + \phi) - s_Q(t)\sin(2\pi f_{rc}t + \phi) \qquad (4.1)$$

where $s_I(t)$ and $s_Q(t)$ are given in Equation (3.18). Note however that in Equation (4.1) we have also taken into account the *actual phase* ϕ of the high-frequency signal oscillators (mixer stage). This is illustrated in Figure 8 for the case when K is odd for which $f_{rc} = f_c$.

To obtain an OFDM signal with sufficient signal power, a power amplifier (PA) is needed. This means that if the amplifier amplifies the input signal amplitude with a factor A then the signal power is changed with a factor A^2.

It should be remembered that an OFDM signal basically equals the summation of K QAM signals, see e.g., Equation (1.13). Therefore, we can expect that there will be time-intervals where the OFDM signal is weak due to ***destructive addition*** of the K signals. In the same way we can expect that there will be time-intervals where the OFDM signal is strong due to ***constructive addition*** of the K signals. Hence, there will be amplitude (envelope) variations in the OFDM signal, and if these variations are too large they will cause some problems concerning the implementation of the power amplifier. The so-called **Peak-to-Average-Power-Ratio** (PAPR, see, e.g., ref. [9]) is a common parameter to quantify the instantaneous power variation in a signal. For signals with high PAPR it is a challenge to implement power-efficient and low-cost power amplifiers, and this is especially important in, e.g., the uplink in mobile communication systems.
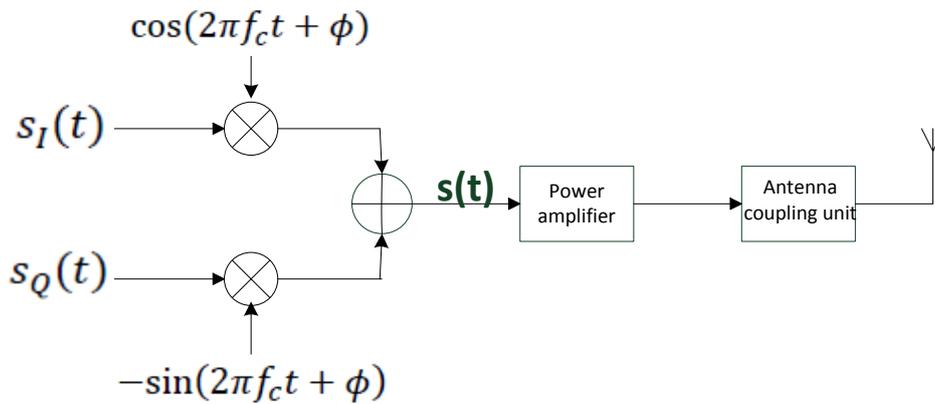
Figure 8. Block diagram illustrating frequency up-conversion (mixer stage) to the carrier frequency (K is odd), the power amplifier, and the antenna coupling unit. The OFDM signal $s(t)$ is given in Equation (4.1).

The last block in Figure 8 is the antenna coupling unit which is the interface to the antenna. Finally, the OFDM signal is radiated from the antenna as an electro-magnetic wave propagating in space.

We have here only briefly mentioned the power amplifier and the antenna. The reader is recommended to study these important parts in more advanced literature.

In the next section we will investigate how the multi-path channel changes the transmitted OFDM signal.

Section 5: The multi-path (linear filter) channel, and the additive white Gaussian noise (AWGN)

The OFDM signal $s(t)$ in Equation (4.1) is amplified and transmitted through a multi-path channel (or a linear filter channel), and in this section we will determine how the transmitted signal is changed by this channel. It is here assumed that the filter can be considered to be time-invariant over a *few OFDM symbol intervals*.

Since the channel is linear it is convenient to first determine how the QAM signal with index k in the OFDM signal is changed by the channel. The result obtained will then also tell us how the remaining K-1 QAM signals are changed by the channel.

Using Equations (3.18) and (4.1) we conclude that the transmitted QAM signal that carries the signal point a_k can be expressed as,

$$A\text{Re}\{a_k e^{j2\pi g_k f_\Delta(t-T_{CP})} e^{j(2\pi f_{rc}t+\phi)}\} = A\text{Re}\{a_k e^{j(2\pi f_k t+\theta_k)}\}, \quad 0 \le t \le T_s \qquad (5.1)$$

and this signal is zero outside the OFDM symbol interval. A denotes the amplitude amplification in the power-amplifier. The sub-carrier frequency is (see also Equation (1.8)) f_k, $f_k = f_{rc} + g_k f_\Delta$, and the phase θ_k in Equation (5.1) is,

$$\theta_k = -\frac{2\pi g_k T_{CP}}{T_{obs}} + \phi \qquad (5.2)$$

The linear filter channel has the (real) impulse response $h(t)$, and its input signal is denoted $q(t)$, see also Figure 9.
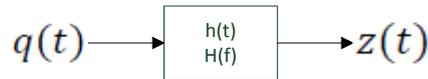
Figure 9. Illustrating a linear filter channel (e.g. a multi-path channel).

In case the linear filter is a multi-path channel with P signal paths its impulse response may be expressed as,

$$h(t) = \sum_{p=1}^{P} \alpha_p \delta(t - \tau_p) \qquad (5.3)$$

If we assume (for simplicity) that the delays in the multi-path channel are numbered in increasing order then we have that $\tau_1 < \tau_2 < \cdots < \tau_P$. Furthermore, in this case it is easy to identify **the duration of the impulse response**, here denoted T_{ch}, to be equal to the largest delay, i.e. $T_{ch} = \tau_P$.

It is also straight-forward to obtain the transfer function $H(f)$ of the multi-path channel in Equation (5.3),

$$H(f) = \int_{-\infty}^{\infty} h(t)e^{-j2\pi ft} dt = \sum_{p=1}^{P} \alpha_p e^{-j2\pi f\tau_p} \qquad (5.4)$$

Let us now investigate the output signal, here denoted $z(t)$, from a channel that can be represented by the impulse response $h(t)$. The assumptions below are made,

- The input signal $q(t)$ is given by Equation (5.1).
- It is assumed that the impulse response $h(t) = 0$ outside the time-interval $0 \leq t \leq T_{ch}$.
- It is assumed that $T_{CP} \geq T_{ch}$ (in practice we also have that $T_s \gg T_{CP}$).

The convolutional integral gives us a way to calculate the output signal $z(t)$,

$$z(t) = \int_{-\infty}^{\infty} h(x)q(t-x)dx = \int_0^{T_{ch}} h(x)q(t-x)dx \tag{5.5}$$

Since the function $q(t)$ equals zero outside the interval $0 \leq t \leq T_s$, the function $q(t-x)$ in Equation (5.5) equals zero outside the interval $(t - T_s) \leq x \leq t$.

The output signal $z(t)$ is therefore zero outside the time-interval $0 \leq t \leq T_s + T_{ch}$. However, to calculate the output signal within this interval it is convenient to study the three sub-intervals below.

$0 \leq t \leq T_{ch}$:

In this time-interval the output signal $z(t)$ in Equation (5.5) is,

$$z(t) = \int_0^t h(x)ARe\{a_k e^{j(2\pi f_k(t-x)+\theta_k)}\}dx \tag{5.6}$$

and this is the ***initial transient*** behavior of the output signal.

$T_{ch} \leq t \leq T_s$:

In this time-interval the output signal $z(t)$ in Equation (5.5) is,

$$z(t) = \int_0^{T_{ch}} h(x)ARe\{a_k e^{j(2\pi f_k(t-x)+\theta_k)}\}dx = ARe\{a_k e^{j(2\pi f_k t+\theta_k)} \int_0^{T_{ch}} h(x)e^{-j2\pi f_k x}dx\} \tag{5.7}$$

Observe that the integral on the right-hand side equals the ***transfer function*** of the filter, evaluated at the sub-carrier frequency f_k, i.e. $H(f_k)$!

Therefore, we can write,

$$z(t) = ARe\{a_k H(f_k)e^{j(2\pi f_k t+\theta_k)}\} \tag{5.8}$$

This result is indeed very important and it should be compared with the input signal in Equation (5.1). Equation (5.8) shows that within the time-interval $T_{ch} \leq t \leq T_s$ *the output signal is also a **QAM** signal*, **but the signal point a_k is distorted** to be $a_k H(f_k)$. Multiplication with $H(f_k) = |H(f_k)|e^{jarg(H(f_k))}$ means that the original signal point a_k is *attenuated* with $|H(f_k)|$ and *phase rotated* with $arg(H(f_k))$.

$T_s \leq t \leq T_s + T_{ch}$:

In this time-interval the output signal $z(t)$ in Equation (5.5) is,

$$z(t) = \int_{t-T_s}^{T_{ch}} h(x)ARe\{a_k e^{j(2\pi f_k(t-x)+\theta_k)}\}dx \tag{5.9}$$

and this is the ***ending transient*** behavior of the output signal.

Now, if the input signal to the filter equals the OFDM signal $As(t)$ where $s(t)$ is given by Equations (3.18) and (4.1) we conclude that the input OFDM signal can be expressed as,

INPUT OFDM: $As(t) = ARe\left\{\left(\sum_{k=0}^{K-1} a_k e^{j2\pi g_k f_\Delta(t-T_{CP})}\right)e^{j(2\pi f_{rc}t+\phi)}\right\}$, $0 \le t \le T_s$ (5.10)

or alternatively as,

INPUT OFDM: $As(t) = ARe\left\{\sum_{k=0}^{K-1} a_k e^{j(2\pi f_k t+\theta_k)}\right\}$, $0 \le t \le T_s$ (5.11)

and this input OFDM signal is zero outside the OFDM symbol interval. The sub-carrier frequency f_k, the phase θ_k and the reference carrier frequency f_{rc} are given in connection to Equation (5.1).

Applying the results in Equations (5.6)-(5.9) to each of the K input QAM signals, and using that $T_{CP} \ge T_{ch}$ we find that **the output signal $z(t)$ is also an OFDM signal in the time-interval $T_{CP} \le t \le T_s$**, where it can be expressed as,

OUTPUT OFDM: $z(t) = ARe\left\{\left(\sum_{k=0}^{K-1} a_k H(f_k)e^{j2\pi g_k f_\Delta(t-T_{CP})}\right)e^{j(2\pi f_{rc}t+\phi)}\right\}$, $T_{CP} \le t \le T_s$ (5.12)

or alternatively as,

OUTPUT OFDM: $z(t) = ARe\left\{\sum_{k=0}^{K-1} a_k H(f_k) e^{j(2\pi f_k t+\theta_k)}\right\}$, $T_{CP} \le t \le T_s$ (5.13)

Furthermore, in the relatively short time-intervals $0 \le t \le T_{CP}$ and $T_s \le t \le T_s + T_{CP}$ the output signal $z(t)$ contains a transient behavior. Note that if the _**next**_ input OFDM signal starts at $t = T_s$ then the corresponding initial output transient will coincide (i.e. overlap) with the ending output transient of the current OFDM signal. This overlap of OFDM signals may cause _**inter-symbol interference**_ in the receiver unless counter-measures are made at the receiver side. As we will see in section 6, a simple solution can be used in the receiver to eliminate the possibility of such inter-symbol interference.

The signal appearing at the receiving antenna (see Figure 10 on page 38) can be expressed as,

$$z(t) + n(t) + \gamma(t) \qquad\qquad (5.14)$$

where $z(t)$ is the desired signal described in Equations (5.12)-(5.13) and in the text just below these equations. The term $n(t)$ in Equation (5.14) is assumed to be *additive white Gaussian noise (AWGN)*. The power spectral density of the random process $n(t)$ equals a constant over the entire frequency axis ("white"), and this constant is denoted $N_0/2$. The signal $\gamma(t)$ in Equation (5.14) represents all other signals that may be present at the receiving antenna. The frequency content of $\gamma(t)$, within the bandwidth occupied by $z(t)$, is assumed to be *virtually zero*. Hence, the only *in-band disturbance* assumed in these lecture notes are in-band noise originating from $n(t)$.

This completes the description of the communication channel studied in these lecture notes. In the next sections we will investigate different steps in the receiver and also show how the K received distorted and noisy signal-points efficiently can be extracted by using the DFT.

A short summary of some basic relationships in Section 5:

- The assumptions for the analysis in this section are given on page 33.
- Observe the important practical consequences of Equations (5.7)-(5.8).
- Observe the initial transient and the ending transient at the output of the channel.
- Compare Equations (5.10)-(5.11) with Equations (5.12)-(5.13)!

Section 6: The Receiver: Frequency down-conversion, sampling (A/D), removal of the CP, and the DFT

The ultimate goal of the receiver is to, as good as possible, recover the sequence of information bits that corresponds to the original sequence of K QAM signal points $a_0, a_1, \dots, a_{K-1}$. To obtain this goal the first sub-goal of the receiver typically is to extract the corresponding K *received distorted and noisy signal points*, and the purpose of this section is to show how the DFT can be used to accomplish this.

The second, and last, sub-goal is to use the sequence of K received distorted and noisy signal points as input to a suitable *decoding algorithm*, see Figure 2 on page 2. The output sequence from the decoding algorithm is the receiver´s decision of the original sequence of information bits that was sent from the transmitter. In these lecture notes decoding algorithms will not be investigated, so the interested reader is recommended to study more advanced literature on this topic.

Before going into details concerning frequency down-conversion to baseband let us start with a fundamental example of how a received noisy QAM signal point may be extracted from a received noisy QAM signal. This example is very important since it gives a good illustration to why the DFT can be used in OFDM receivers to extract the K received noisy signal points.

In this **example** we assume that the received signal $r(t)$ equals (compare with Equation (1.4)),

$$r(t) = b_I \cos(2\pi f_B t) - b_Q \sin(2\pi f_B t) + n(t), \ 0 \leq t \leq T \tag{6.1}$$

Hence, the received signal is a single QAM signal disturbed by AWGN, and our goal in this example is to show how to extract the received noisy signal point. Basic decision theory tells us that in this case the receiver should use two orthonormal basis functions, here denoted $\psi_1(t)$ and $\psi_2(t)$. These (real) functions should satisfy the two conditions,

$$\int_0^T \psi_1(t)\psi_2(t) \, dt = 0 \qquad \text{(orthogonal)} \tag{6.2}$$

$$\int_0^T \psi_1(t)^2 \, dt = \int_0^T \psi_2(t)^2 \, dt = 1 \quad \text{(normalization)} \tag{6.3}$$

In this example the choice of orthogonal basis functions are,

$$\psi_1(t) = \cos(2\pi f_B t)/C, \qquad 0 \leq t \leq T \tag{6.4}$$

$$\psi_2(t) = -\sin(2\pi f_B t)/C, \qquad 0 \leq t \leq T \tag{6.5}$$

where C is a normalization constant chosen such that Equation (6.3) is satisfied. It is also assumed that f_B and T are such that Equation (6.2) is satisfied.

The received noisy signal point consists of two coordinates since a QAM signal is assumed in this example. The first coordinate, denoted r_1, is the correlation between the received signal and the first basis function,

$$r_1 = \int_0^T r(t)\psi_1(t) \, dt = Cb_I + n_1 \tag{6.6}$$

and the second coordinate is calculated in a similar way,

$$r_2 = \int_0^T r(t)\psi_2(t) \, dt = Cb_Q + n_2 \tag{6.7}$$

In Equations (6.6)-(6.7) n_1 and n_2 denotes non-desired noise contributions from the AWGN $n(t)$. It can be shown that these two noise contributions each have a Gaussian probability density function, zero mean and variance $N_o/2$. Furthermore, they are also independent. Note that Equations (6.6)-(6.7) may be interpreted as frequency down-conversion to baseband.

The two values (r_1, r_2) in Equations (6.6)-(6.7) ***define the received noisy signal point*** and they are of *fundamental importance* in the decision process.

Let us now express the complex value r in the following way,

$$r = r_1 + jr_2 = \int_0^T r(t)e^{-j2\pi f_B t}\, dt / C = R(f_B)/C = Cb + n \tag{6.8}$$

where $b = b_I + jb_Q$ and $n = n_1 + jn_2$.

It is now very important to observe in Equation (6.8) that **the received noisy signal point r can be found by calculating the Fourier transform $R(f)$ of the received signal $r(t)$ over the time interval $0 \leq t \leq T$, and then sample $R(f)$ at $f = f_B$ to obtain $R(f_B)$.** As will be seen later on, *using the DFT in an OFDM receiver can be viewed as a natural extension of this result*.

It is now time to focus on frequency down-conversion to baseband.

Frequency down-conversion to baseband:

The input signal to the receiving antenna is given in Equation (5.14) on page 34, and the first part of the receiver is illustrated in Figure 10 on the next page. It is seen in Figure 10 that the antenna coupling unit is followed by a band-pass (BP) filter. This filter may have a relatively large pass-band to allow for several frequency bands that might be of interest to the receiver, e.g. the OFDM frequency band that contains the signal $z(t)$ in Equation (5.13). Signals located outside the pass-band of the band-pass filter are rejected (more attenuated) and are of no interest to the receiver.

The received signal is normally a very weak signal and it needs to be amplified. However, with weak signals additional noise can be very hurtful to the *signal-to-noise-ratio*, and therefore a *low-noise amplifier* (LNA) is used in the receiver. LNA:s are designed with the purpose to keep the internal generated noise to a minimum, and only a very small loss in signal-to-noise ratio due to the LNA is acceptable.

It is *in principle* possible to extract the K received distorted and noisy signal points directly from the output signal of the LNA, here denoted $y_r(t)$. We learned from the previous example in this section, see Equation (6.8), that the received distorted and noisy signal point with index k is found if we evaluate the Fourier transform of $y_r(t)$ at $f = f_k$, i.e., if we calculate the value

$$\int_{T_{CP}}^{T_s} y_r(t)e^{-j2\pi f_k t}\, dt, \qquad k = 0,1,\dots,K-1 \tag{6.9}$$

Since the sub-carrier frequency separation is $f_\Delta = 1/T_{obs}$ and since the sub-carrier frequency f_k is at a high frequency, different QAM-signals are virtually orthogonal, see Equation (1.19), and this implies that there will be no "leakage" from the other (K-1) QAM-signals in the value given by Equation (6.9).

However, instead of doing the calculations at high frequencies as in Equation (6.9) it is, as we will see, much more practical and efficient to do the calculations in baseband, and especially in the digital domain by using the DFT. This means that we need to create a baseband spectrum from the high frequency OFDM spectrum that is contained in the signal $y_r(t)$.

Let us use the reference frequency f_{rc} of the received OFDM signal in the demodulation process, and we know from section 1 that $f_{rc} = f_{k_{rc}}$.

Frequency down-conversion is illustrated in Figure 10 for the case when K is odd for which $f_{rc} = f_c$. It is seen in this figure that the LNA is followed by multipliers and low pass filters, and this part is referred to as *homodyne* reception. **The goal of homodyne reception is frequency down-conversion to baseband and thereby obtain the desired baseband components**, denoted $r_I(t)$ and $r_Q(t)$, such that,

$$R_I(f) + jR_Q(f) = Y_r(f + f_{rc}), \qquad |f| \le W_{lp} \tag{6.10}$$

where W_{lp} denotes the baseband cut-off frequency (bandwidth) of each low-pass filter in Figure 10.

$$\cos(2\pi f_c t + \phi_r)$$

$$-\sin(2\pi f_c t + \phi_r)$$
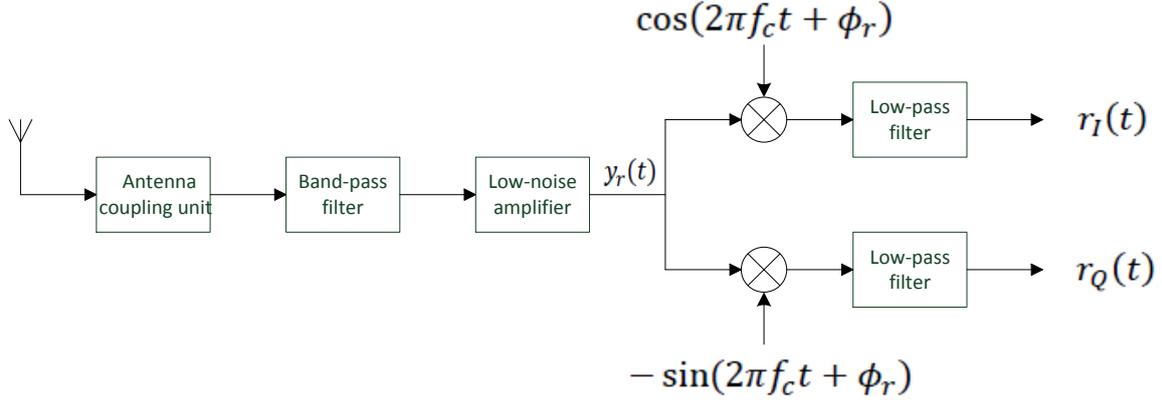
Figure 10. Illustrating the first part of the receiver: the antenna coupling unit, band-pass filter, low-noise amplifier (LNA) and a homodyne unit for frequency down-conversion and extracting the baseband signals $r_I(t)$ and $r_Q(t)$. It is here assumed that K is odd for which $f_{rc} = f_c$.

The output signal $y_r(t)$ from the LNA in Figure 10 may contain several applications located in different frequency bands, but the receiver is here only interested in the frequency band that contains the desired OFDM signal $z(t)$.

We know the reference carrier frequency f_{rc} and the approximate bandwidth Kf_Δ of the desired signal $z(t)$ in Equation (5.13) on page 34. Therefore, the frequency of the oscillator signals in Figure 10 should be tuned to f_{rc} Hz and the bandwidth W_{lp} of the low pass filters should be approximately $W_{lp} \approx Kf_\Delta/2$ Hz. In Figure 10, the actual phase of the high-frequency oscillator signals is denoted ϕ_r.

Now let $r_1(t)$ denote **only** the part of the signal $y_r(t)$ that occupies the same part of the spectrum as the desired OFDM signal does. This means that the signal $(y_r(t) - r_1(t))$ has no frequency components within the approximate frequency range $f_{rc} - \frac{Kf_\Delta}{2} \leq f \leq f_{rc} + \frac{Kf_\Delta}{2}$, and the signal $(y_r(t) - r_1(t))$ will therefore (ideally) not contribute to the signals $r_I(t)$ and $r_Q(t)$ in Figure 10, only the signal $r_1(t)$ will.

So, the high-frequency signal $r_1(t)$ is therefore important and it can be expressed as,

$$r_1(t) = Re\{(r_{1,I}(t) + jr_{1,Q}(t))e^{j2\pi f_{rc}t}\} \tag{6.11}$$

where, using Equation (5.12), the corresponding complex baseband signal is found to be,

$$r_{1,I}(t) + jr_{1,Q}(t) = A\sum_{k=0}^{K-1} a_k H(f_k)e^{j2\pi g_k f_\Delta(t-T_{CP})}e^{j\phi} G_1(f_k) + n_1(t), \quad T_{CP} \leq t \leq T_s \tag{6.12}$$

The frequency function $G_1(f_k)$ represents the combined effect of the band-pass filter and the LNA on the QAM signal with index k, and the complex signal $n_1(t)$ represents "white" baseband noise (assuming that $|G_1(f)|$ is constant within the OFDM spectrum).

Let us now, for convenience, assume that the two low-pass filters in Figure 10 are almost ideal, i.e. it is here assumed that the transfer function of each filter is constant within the approximate frequency range $-Kf_\Delta/2 \leq f \leq Kf_\Delta/2$, and has a high attenuation at all other frequencies.

By studying the homodyne part in Figure 10, and also using Equation (6.11), we conclude that the two outputs $r_I(t)$ and $r_Q(t)$ from the low-pass filters can be determined from the relationship below,

$$r_I(t) + jr_Q(t) = [\,r_1(t)e^{-j(2\pi f_{rc}t + \phi_r)}]_{LP} = [Re\{(r_{1,I}(t) + jr_{1,Q}(t))e^{j2\pi f_{rc}t}\}e^{-j(2\pi f_{rc}t + \phi_r)}]_{LP} \quad (6.13)$$

where the notation $[c(t)]_{LP}$ means "baseband (or low-frequency) component of $c(t)$".

The reader is recommended to start with the right-hand side of Equation (6.13) and show that,

$$r_I(t) + jr_Q(t) = \frac{(r_{1,I}(t) + jr_{1,Q}(t))e^{-j\phi_r}}{2} \circledast g_{lp}(t) \quad (6.14)$$

where the symbol $\circledast$ in Equation (6.14) denotes convolution, and $g_{lp}(t)$ denotes the impulse response of each low-pass filter (the transfer function is denoted $G_{lp}(f)$). Combining Equations (6.12) and (6.14), we obtain the **important result**,

$$r_I(t) + jr_Q(t) = \sum_{k=0}^{K-1} a_k H_{eq}(f_k)e^{j2\pi g_k f_\Delta(t-T_{CP})} + w(t), \quad T_{CP} \leq t \leq T_s \quad (6.15)$$

Observe that a so-called "***equivalent channel***" $H_{eq}(f_k)$ is introduced in Equation (6.15), and the noise is represented by the complex signal $w(t)$ (assumed to be "white" baseband noise).

The "equivalent channel" is a very important and convenient concept since it represents the combined effect of all sub-blocks in the complete communication chain. Mathematically, we have from Equations (6.12) and (6.14) that,

$$H_{eq}(f_k) = H_{eq,k} = AH(f_k)e^{j\phi}G_1(f_k)e^{-j\phi_r}G_{lp}(f_k - f_{rc} = g_k f_\Delta)/2 \quad (6.16)$$

It is seen in Equations (6.15)-(6.16) that $H_{eq}(f_k)$, alternatively $H_{eq,k}$, includes, e.g., the physical channel filter model, the band-pass filter, the LNA, and the low-pass filters. Since $H_{eq,k} = |H_{eq,k}|e^{jarg(H_{eq,k})}$ the phase $arg(H_{eq,k})$ may also include (absorb) a phase-component that is a consequence of the specific description used in Equation (6.15).

Note that for the result in Equation (6.15) to be valid, the duration of the *overall impulse response* should not exceed T_{CP} (compare with Equation (5.7)). Another way to rephrase this is to say that if virtually all of the energy in the overall impulse response is contained within the time-interval $0 \leq t \leq T_{CP}$, then Equations (6.15)-(6.16) are sufficiently accurate, and this is typically the case in well-designed communication systems.

Observe also that the description in Equation (6.15) is independent of the specific implementation of the OFDM signal at the transmitter side.

From Equations (6.15)-(6.16) it is concluded that $H_{eq,k}$ represents the overall attenuation and rotation of the original signal point a_k. **Hence, the original signal point a_k is distorted and it appears as $a_k H_{eq,k}$ at the receiver side**. Therefore, as we will see, the value $a_k H_{eq,k}$ is a very important component in the corresponding received noisy signal point. In most cases the physical channel filter $H(f)$ causes *random* and *frequency dependent* attenuation and rotation, so called ***fading***. Hence, the sent K QAM signals may then be treated differently by the channel (concerning attenuation and rotation).

In case the remaining blocks in the communication chain overall act as a frequency independent complex constant, denoted B, then we have $H_{eq,k} = H(f_k)B$.

Instead of calculating Equation (6.9) to obtain the received distorted and noisy signal point with index k we can calculate the Fourier transform of the complex signal $(r_I(t) + jr_Q(t))$ in Equation (6.15), and evaluate this Fourier transform at the baseband sub-carrier frequency $f = f_k - f_{rc} = g_k f_\Delta$. The reason for this is the frequency shift down to baseband that is performed by the homodyne unit (see Equation (6.10) on page 37), which implies that the spectral characteristics of the high-frequency signal $r_1(t)$ at the high frequency f_k Hz will, except for the factor $e^{-j\phi_r}$ in Equation (6.14) and the influence of $G_{lp}(g_k f_\Delta)$, be the same as the spectral characteristics of the low-frequency signal $(r_I(t) + jr_Q(t))$ at the baseband frequency $(f_k - f_{rc}) = g_k f_\Delta$ Hz. However, as we will see, the DFT will instead be used to extract the K received distorted and noisy signal points.

It should also be mentioned here that most decoding algorithms need knowledge about the overall channel parameters $H_{eq,k}$, $k = 0,1, \dots (K-1)$. Therefore, a ***channel estimation algorithm*** is needed in the receiver. The result of this algorithm will be channel parameter estimates. Normally, completely known so-called pilot-symbols or channel-reference symbols are transmitted at specific sub-carriers and in specific OFDM symbol intervals in the OFDM time-frequency grid. Based on the received signal at the corresponding sub-carrier and OFDM interval, the corresponding channel parameter can be estimated. From all these specific estimates (two-dimensional "samples") it is possible to reconstruct an estimate of the two-dimensional channel filter, and thereby obtain estimates of $H_{eq,k}$, $k = 0,1, \dots (K-1)$ over *several* say P consecutive OFDM symbol intervals. In these lecture notes we will not analyze any channel estimation algorithms, so the interested reader is recommended to study more advanced literature on this topic.

This completes the description of the analog part of the receiver in Figure 10. In the next sub-section we will study the transition to the digital domain by assuming ideal sampling (A/D).

Sampling (A/D) and removal of the CP:

In this sub-section only ideal A/D converters are considered and by this we mean *instantaneous sampling* and *infinite precision* in the samples. See also Figure 11 on the next page. As an example, consider ideal sampling of the signal $r_I(t)$ at $t = t_0$. With infinite precision the value obtained is then $r_I(t_0)$, in contrast to if finite precision is used where a *quantized* value of $r_I(t_0)$ instead is the result (and it is represented by a finite number of bits). In practice A/D converters are non-ideal, and efficient "close to ideal" A/D converters are non-trivial to implement. However, in these lecture notes we assume that the non-ideal A/D converters are fast and accurate enough such that we may approximate them with ideal A/D converters.

One goal in this sub-section is to obtain sampled versions of the two signals $r_I(t)$ and $r_Q(t)$ in Figures 10-11. Using the same arguments that was used in step 2 in Section 2, we conclude that the *sampling frequency* f_{samp} may be chosen as $f_{samp} = Nf_\Delta$ samples per second, and N should be chosen larger than K (compare with Equation (2.12)), and large enough such that the sampling theorem can be considered to be sufficiently fulfilled. Observe that the choice of N to use in the receiver is a decision of the *engineers of the receiver*, and it does **not** need to be the same value as was chosen at the transmitter side (which typically is unknown in many cases). In general, how the transmitted OFDM signal was created may not be known at the receiver side (consider, e.g., the up-link in a multi-user mobile communication application).

Corresponding to the current OFDM interval $0 \leq t \leq T_s$, the two sequences of samples generated from the A/D converters in Figure 11 are $r_I(mT_{obs}/N)$ and $r_Q(mT_{obs}/N)$, respectively, $m = 0,1, \dots, (L + N - 1)$.

Note however that the first L samples (the CP) will here not be used in the detection process and these samples are therefore *ignored* in the future, see Figure 11!

This means that the signal interval where an overlap between OFDM signals may occur is ignored by the receiver, and thereby **possible inter-symbol interference between OFDM signals is eliminated in the receiver** (provided that $T_{ch} \leq T_{CP}$), see also Section 5. Since the CP is assumed to be much smaller than T_s the loss of ignoring the CP is here assumed to be acceptable.

The remaining N samples (after removal of the CP) represent the receiver's observation interval and they are extremely important. These samples are collected in the two vectors $\boldsymbol{r}_I$ and $\boldsymbol{r}_Q$ defined below (see also Figure 11),

$$r_{I,n} = r_I((L + n)T_{obs}/N), \quad n = 0,1, \dots, N - 1 \tag{6.17}$$

$$r_{Q,n} = r_Q((L + n)T_{obs}/N), \quad n = 0,1, \dots, N - 1 \tag{6.18}$$

We now create the complex size-N vector $\boldsymbol{r}$ as,

$$\boldsymbol{r} = \boldsymbol{r}_I + j\boldsymbol{r}_Q \tag{6.19}$$

From Equation (6.15) on page 39 it is seen that *the discrete-time signal $\boldsymbol{r}$ contains samples of the complex baseband signal $x_r(t)$*, where $x_r(t)$ is defined as,

$$x_r(t) = r_I(t + T_{CP}) + jr_Q(t + T_{CP}) = \sum_{k=0}^{K-1} a_k H_{eq,k} e^{j2\pi g_k f_\Delta t} + w'(t), \quad 0 \leq t \leq T_{obs} \tag{6.20}$$

41

The signal $x_r(t)$ in Equation (6.20) should be compared with the signal $x(t)$ in Equation (2.3) on page 9.

Observe in Equation (6.20) that the effects of the complete communication chain are that the original signal point a_k is changed (distorted) to $a_k H_{eq,k}$, $k = 0, 1, \dots (K-1)$, and that Gaussian baseband noise is present in the corresponding complex baseband OFDM signal $x_r(t)$ at the receiver side.
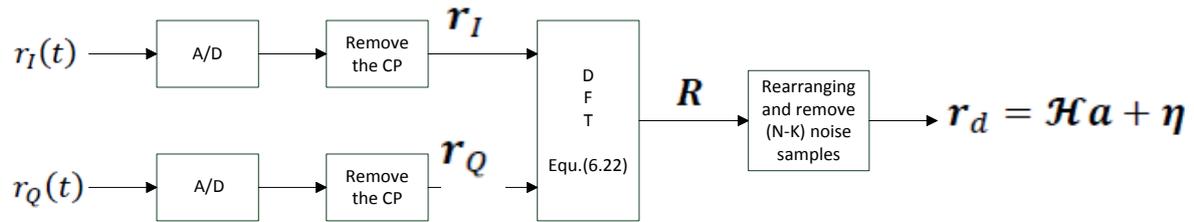
Figure 11. Illustrating sampling, removal of the CP, and the size-N DFT in the receiver to extract the K received distorted and noisy signal points collected in the size-K vector r_d.

Using the DFT:

The remaining investigation of the receiver aims to extract the K received distorted and noisy signal points. The received signal point carried by the high-frequency subcarrier frequency f_k can be found by calculating the Fourier transform of the signal $x_r(t)$ in Equation (6.20) at the corresponding baseband sub-carrier frequency $g_k f_\Delta$ Hz. However, to efficiently obtain the K received distorted and noisy signal points with the size-N DFT, let us continue as follows.

Consider the Fourier transform of the discrete-time signal r in equation (6.19),

$$R(v) = \sum_{n=0}^{N-1} r_n e^{-j2\pi v n} \tag{6.21}$$

Remember from, e.g., Figure 6 on page 17 that $R(v)$ is periodic in v with period 1. Furthermore, the Fourier transform of the signal $x_r(t)$ in Equation (6.20) appears as a very significant part of $R(v)$ within the fundamental interval $-1/2 \le v \le 1/2$, see Equation (2.17), and the example in connection to Figure 5 on page 15.

As has been pointed out several times the K received distorted and noisy signal points can be extracted by calculating the Fourier transform at K specific frequencies, i.e. by ***sampling the Fourier transform*** at K specific frequencies.

Since the DFT results in frequency-domain samples it is very well suited for extracting the desired signal points.

Let us therefore calculate the size-N DFT of the discrete-time signal r,

$$R_m = R(v = m/N) = \sum_{n=0}^{N-1} r_n e^{-j2\pi mn/N}, \quad m = 0,1,\dots,N-1 \tag{6.22}$$

In practice, **N is chosen to be a power of 2** since fast Fourier transform (FFT) algorithms can then be used to significantly speed up the calculations in Equation (6.22).

In Figure 11 on the previous page the size-N column vector R contains the frequency-domain samples R_m.

Observe that the frequency-domain sample R_m is obtained at the normalized frequency (compare with Figure 6 on page 17),

$$v = \frac{m}{N} = \frac{m f_\Delta}{N f_\Delta} \tag{6.23}$$

By comparing the frequency-domain sample R_m with the frequency-domain sample X_m obtained in Section 2, we conclude that the sample R_0 contains the value $a_{k_{rc}} H_{eq,k_{rc}}$, and that the sample R_{N-1} contains the value $a_{(k_{rc}-1)} H_{eq,(k_{rc}-1)}$.

To be more precise we can express R as,

$$R = X_r + w_r \tag{6.24}$$

where X_r is the noise-free part of R, and w_r is the noise vector.

Let us also introduce the size-K column vector $\mathcal{H}a$, where a is the size-K column vector containing the K original QAM symbols. $\mathcal{H}$ is a size KxK matrix containing the equivalent channel parameters $H_{eq,k}$ on the main diagonal, and the off-diagonal elements are equal to zero.

This means that,

$$(\mathcal{H}a)^{tr} = (a_0 H_{eq,0} \; a_1 H_{eq,1} \; .... \; a_{K-1} H_{eq,K-1}) \tag{6.25}$$

Hence, the size-K column vector $\mathcal{H}a$ contains *the K noise-free received distorted signal points.*

By comparing with the general results obtained in Section 2 we deduce that X_r in Equation (6.24) is a "rotated" version of $\mathcal{H}a$, or more precisely from Equation (2.31) on page 20.

$$X_r = N Q_t \mathcal{H} a \tag{6.26}$$

As **examples**, the first value in X_r is $X_{r,0}$, which is contained in the frequency-domain sample $R_0 = R(v = 0)$, equals $X_{r,0} = N a_{k_{rc}} H_{eq,k_{rc}}$. The last value in X_r is $X_{r,(N-1)}$, which is contained in the frequency-domain sample $R_{N-1} = R\left(v = \frac{N-1}{N}\right)$, equals $X_{r,(N-1)} = N a_{(k_{rc}-1)} H_{eq,(k_{rc}-1)}$.

From Equation (6.24) the output size-N vector R from the DFT can then be expressed as,

$$R = N Q_t \mathcal{H} a + w_r \tag{6.27}$$

To recover the K received distorted and noisy signal points we "re-rotate" the vector R according to Equation (2.34) on page 21,

$$r_d = \frac{1}{N} Q_r R = Q_r Q_t \mathcal{H} a + \frac{1}{N} Q_r w_r = \mathcal{H} a + \eta \tag{6.28}$$

Observe that the elements in the size-K column vector r_d in Equation (6.28) are the desired received distorted and noisy signal points,

$$r_{d,k} = a_k H_{eq,k} + \eta_k, \quad k = 0,1, ..., (K-1) \tag{6.29}$$

where η_k denotes additive complex Gaussian noise. Note also that the operation in Equation (6.28) automatically ignores the (N-K) positions in R that contain only out-of-band noise.

The results in Equations (6.28)-(6.29) are extremely important! See also Figure 11 on page 42.

The next step in the receiver is to feed the vector r_d to the decoding unit (compare with Figure 2 on page 2). However, decoding algorithms are not covered in these lecture notes.

For the special case of *uncoded* OFDM (though rarely used in practice) we should decode each attenuated and rotated square QAM signal constellation separately. In this case it is well known that ML symbol decoding of the n:th M_n- ary QAM signal constellation (square) is based only on $r_{d,n}$ and it yields the symbol error probability $P_{s,k}$ equal to,

$$P_{s,k} = 4\left(1 - \frac{1}{\sqrt{M_k}}\right)Q\left(\sqrt{\frac{d^2_{min,k}\mathcal{E}_{b,k}}{N'_{0,k}}}\right) - 4\left(1 - \frac{1}{\sqrt{M_k}}\right)^2 Q^2\left(\sqrt{\frac{d^2_{min,k}\mathcal{E}_{b,k}}{N'_{0,k}}}\right), \quad k = 0,1\dots,K-1 \quad (6.30)$$

where $d^2_{min,k}$ is the normalized squared minimum Euclidean distance in the received QAM signal constellation with index k and,

$$d^2_{min,k} = \frac{3log_2(M_k)}{M_k - 1} \tag{6.31}$$

Furthermore, $\mathcal{E}_{b,k}$ denotes the average received signal energy per information bit in the received QAM signal space with index k, and $\mathcal{E}_{b,k}$ is proportional to $|H_{eq,k}|^2$. The variance of the noise, in each dimension in the two-dimensional signal space with index k, is here $N'_{0,k}/2$.

In the next sections we will take a look at some alternative implementations that are possible in case the sampling frequency is approximately at least twice as high as the sampling frequency used so far in these lecture notes (assuming the same values of K and f_Δ) .

A short summary of some basic relationships in Section 6:

- Observe in Equation (6.8) that the received noisy signal point r can be found by calculating the Fourier transform $R(f)$ of the received signal $r(t)$ over the time interval $0 \le t \le T$, and then sample $R(f)$ at $f = f_B$ to obtain $R(f_B)$.
- Figure 10 on page 38 illustrates the first part of the receiver, including the homodyne unit.
- Observe the result in Equation (6.15), and also the concept "equivalent channel" parameter on page 39.
- Figure 11 on page 42 illustrates sampling, removal of the CP, and the size-N DFT.
- After removal of the CP, the relationships defined by Equations (6.17)-(6.20) are obtained.
- The size-N output sequence **R** from the DFT can be described by Equation (6.27).
- After "re-rotation" the final desired result is obtained, see Equations (6.28)-(6.29) and Figure 11. ***This result, i.e. the K complex values in the vector r_d, is extremely important*** and it is delivered to the decoding unit in Figure 2 on page 2.

Section 7: An alternative transmitter implementation

In this section we will study an alternative implementation of the transmitter that is possible if the sampling frequency is approximately at least twice as high than the sampling frequency used in Sections 2-4 (where $f_{samp} = Nf_\Delta > Kf_\Delta$) if the same K and f_Δ are used. A higher sampling frequency normally implies a higher cost, e.g., for D/A converters. However, as we will see, interesting and useful alternative implementations can then be obtained. The description given here is to a large extent influenced by the description in ref. [2].

Let us repeat the description of an OFDM signal in the time-interval $0 \le t \le T_s$ according to Equation (1.13),

$$OFDM\ signal(t) = g_{rec}(t)Re\{\textstyle\sum_{k=0}^{K-1} a_k e^{j2\pi f_k t}\} \tag{7.1}$$

The frequency content, for positive frequencies, is roughly indicated in Figure 3a on page 10. A significant difference however, compared to Sections 2-4 is that here we assume that the K sub-carrier frequencies in the OFDM signal in Equation (7.1) have relatively **low frequencies**. More specifically it is here assumed that the sub-carrier frequency f_k equals,

$$f_k = (N_g + k)f_\Delta, \qquad k = 0,1,\dots,K-1 \tag{7.2}$$

where N_g ($N_g \ge 1$) is an integer design parameter and it is typically relatively small. One purpose of the parameter N_g may be to have a suitable guard band in the frequency domain around $f = 0$, e.g., to simplify filtering (this will be more clear later in this section). In case a higher over-all carrier frequency is desired frequency up-conversion as illustrated in Figure 12 on page 49 may be used.

We start the synthesis process with the OFDM signal $s(t)$ in Equation (7.3) below which is defined within the time-interval $0 \le t \le T_{obs}$,

$$s(t) = g_{rec}(t)Re\{\textstyle\sum_{k=0}^{K-1} a_k e^{j2\pi f_k t}\} = \frac{g_{rec}(t)}{2}(\textstyle\sum_{k=0}^{K-1} a_k e^{j2\pi f_k t} + \sum_{k=0}^{K-1} a_k^* e^{-j2\pi f_k t}) \tag{7.3}$$

and **the bandwidth** of $s(t)$, including the N_g unused sub-carriers, **is approximately equal to** $(N_g + K)f_\Delta$ **Hz.**

Let us now determine N time-domain real samples of the real signal $s(t)$ in Equation (7.3) within the time interval $0 \le t \le T_{obs}$ (compare with Section 2). From the description in Equations (7.2)-(7.3), we find that **the sampling frequency** can be chosen as $f_{samp} = Nf_\Delta$ where,

$$f_{samp} = Nf_\Delta > 2(N_g + K)f_\Delta \tag{7.4}$$

Hence, the sampling frequency in this section is approximately *at least twice as high* as in Sections 2-4 (for the same values of K and f_Δ).

Let the vector $\boldsymbol{s}$ contain the N real samples $s_0, s_1, \dots, s_{N-1}$ of the real signal $s(t)$, where

$$s_n = s(nT_{obs}/N) = \frac{1}{2}(\textstyle\sum_{k=0}^{K-1} a_k e^{j2\pi(N_g+k)f_\Delta nT_{obs}/N} + \sum_{k=0}^{K-1} a_k^* e^{-j2\pi(N_g+k)f_\Delta nT_{obs}/N}) \tag{7.5}$$

Observe now that the multiplication (or scaling) factor ½ that appears in Equation (7.5) will be *ignored* below. It is assumed that this can be compensated for later in the transmitter chain, e.g., in the power amplifier (PA).

The expression in Equation (7.5) can then be expressed as,

$$s_n = s\left(\frac{nT_{obs}}{N}\right) = \sum_{k=0}^{K-1} a_k e^{\frac{j2\pi(N_g+k)n}{N}} + \sum_{k=0}^{K-1} a_k^* e^{-\frac{j2\pi(N_g+k)n}{N}} =$$

$$= \sum_{k=0}^{K-1} a_k e^{\frac{j2\pi(N_g+k)n}{N}} + \sum_{k=0}^{K-1} a_k^* e^{-\frac{j2\pi(N_g+k-N)n}{N}} =$$

$$= \sum_{m=N_g}^{N_g+K-1} a_{m-N_g} e^{\frac{j2\pi mn}{N}} + \sum_{m=N-N_g-K+1}^{N-N_g} a_{N-N_g-m}^* e^{\frac{j2\pi mn}{N}}, \qquad n = 0,1,\dots,(N-1)$$

$$(7.6)$$

Continuing as in Section 2, we need the Fourier transform $S(\nu)$ of the discrete-time signal $\boldsymbol{s}$ in Equation (7.6), and $S(\nu)$ is defined by,

$$S(\nu) = \sum_{n=0}^{N-1} s_n e^{-j2\pi\nu n} \tag{7.7}$$

We are especially interested in the frequency-domain samples S_m of $S(\nu)$, given by the size-N DFT,

$$S_m = S(\nu = m/N) = \sum_{n=0}^{N-1} s_n e^{-j2\pi mn/N}, \quad m = 0,1,\dots,N-1 \quad \textbf{(DFT)} \tag{7.8}$$

It should be observed that since the discrete-time signal $\boldsymbol{s}$ is real there are ***symmetries*** in its Fourier transform $S(\nu)$.

As in Section 2, we need to specify the size-N sequence of frequency-domain samples $S_0, S_1, \dots, S_{N-1}$ since this sequence will be used as input sequence to the size-N IDFT to create the desired sequence of time-domain samples $\boldsymbol{s}$.

Note that we may express N as,

$$N = 2(N_g + K) - 1 + N_x \tag{7.9}$$

where $N_x \geq 0$ is a number of zero-valued samples S_m (determined by the choice of N), and the N_x zero-valued samples are located symmetrically around $\nu = 1/2$. A relatively large value of N_x may simplify the filtering operation in the D/A converter in order to extract the fundamental frequency interval $-f_{samp}/2 \leq f \leq f_{samp}/2$, see also Section 3.

If we compare with the situation treated in Section 2, and also use the final expression in Equation (7.6), it is concluded from Equation (7.6) that the frequency-domain samples $S_0, S_1, \dots, S_{N-1}$ can be specified as:

For $N_g \leq m \leq N_g + K - 1$ we find that S_m is,

$$S_{N_g+k} = Na_k, \ 0 \leq k \leq K - 1 \tag{7.10}$$

For $(N - (N_g + K - 1)) \leq m \leq (N - N_g)$ we find that S_m is,

$$S_{N-(N_g+K-1)+k} = Na^*_{K-1-k}, \quad 0 \leq k \leq K - 1 \tag{7.11}$$

The remaining $(N - 2K)$ samples in the sequence $S_0, S_1, \dots, S_{N-1}$ are all equal to zero.

Consider as an **example** the case K=3, $N_g = 2$ and N=12. In this case the desired sequence $S_0, S_1, \dots, S_{11}$ then equals: $0, 0, Na_0, Na_1, Na_2, 0, 0, 0, Na^*_2, Na^*_1, Na^*_0, 0$. Here, $N_x = 3$.

Consider a similar **example** where K=3, $N_g = 2$ and N=11. In this case the desired sequence $S_0, S_1, \dots, S_{10}$ then equals: $0, 0, Na_0, Na_1, Na_2, 0, 0, Na^*_2, Na^*_1, Na^*_0, 0$. Here, $N_x = 2$.

Hence, the size-N sequence of frequency-domain samples $S_0, S_1, \dots, S_{N-1}$ is now completely determined and the desired size-N sequence of time-domain real samples $\boldsymbol{s}$ is created using the size-N IDFT,

$$s_n = \frac{1}{N}\sum_{m=0}^{N-1} S_m e^{j2\pi mn/N}, n = 0, 1, \dots, N - 1 \quad \textbf{(IDFT)} \tag{7.12}$$

In practice, **N is chosen to be a power of 2** since fast Fourier transform (FFT) algorithms can then be used to significantly speed up the calculations in Equation (7.12). See also Figure 12 on page 49.

To create the CP we proceed in the same way as in Section 3. Therefore, if we for a moment allow the definition of the signal $s(t)$ in Equation (7.3) to be valid for all t, then it is seen that the signal construction of $s(t)$ is such that $s(t)$ is **periodic** in t with period T_{obs}, i.e. $s(t) = s(t + T_{obs})$. This means, e.g., that $s(-t_1) = s(T_{obs} - t_1)$.

We now want to preserve the OFDM signal properties in the N time-domain samples that represent $s(t)$, but over an **extended** period of time. This can conveniently be done by using the inherent periodicity in $s(t)$ discussed above. Hence, let us therefore construct a new size-(L+N) vector $\boldsymbol{u}$ as a so-called *periodic extension* of the size-N vector $\boldsymbol{s}$. This means that *the L last samples in $\boldsymbol{s}$ are copied and placed as the first L samples in $\boldsymbol{u}$*. The remaining N samples in $\boldsymbol{u}$ are identical to $\boldsymbol{s}$. This means that,

$$u_0 = s_{N-L}, \dots, u_{L-1} = s_{N-1}, u_L = s_0, \dots, u_{L+N-1} = s_{N-1}. \tag{7.13}$$

The construction of the vector $\boldsymbol{u}$ above implies that the first L samples in $\boldsymbol{u}$ are identical with the last L samples in $\boldsymbol{u}$, and this reflects the periodicity discussed above.

The duration of the OFDM signal interval is T_s, and it can be expressed as,

$$T_s = \frac{(L+N)T_{obs}}{N} = T_{CP} + T_{obs} \tag{7.14}$$

The vector $\boldsymbol{u}$ in Equation (7.13) contains (L+N) real samples of a real OFDM signal defined over the entire OFDM signal interval $0 \leq t \leq T_s$. This OFDM signal is here denoted $u(t)$, where $u(t)$ is a delayed version of the expression that defines the signal $s(t)$ in Equation (7.3), or more precisely,

$$u(t) = g_{rec}(t)Re\left\{\sum_{k=0}^{K-1} a_k e^{j2\pi f_k(t-T_{CP})}\right\}, \quad 0 \leq t \leq T_s \quad (7.15)$$

and $u(t)$ equals zero outside this interval. Furthermore, the m:th sample in the real vector $\boldsymbol{u}$ is,

$$u_m = u(mT_{obs}/N), \quad m = 0,1,\dots,(L+N-1) \quad (7.16)$$

The final operation is to send the real sequence $\boldsymbol{u}$ to a D/A converter (compare with Section 3), and the ideal output from the D/A will be the desired OFDM signal $u(t)$, see Figure 12. Note that only a single D/A converter is needed here, but on the other hand it operates with approximately at least twice as high sampling frequency compared to the sampling frequency used in Sections 2-4 (for the same values of K and f_Δ).

The overall carrier frequency $f_{c,u}$ of the created OFDM signal $u(t)$ is,

$$f_{c,u} = f_0 + \frac{K-1}{2}f_\Delta = (N_g + \frac{K-1}{2})f_\Delta \quad (7.17)$$

and typically $f_{c,u}$ is a relatively low frequency.

In case the OFDM signal $u(t)$ needs to be up-converted to a higher overall carrier frequency f_c, mixing and filtering according to Figure 12 is a possibility. The local oscillator frequency f_l used in the mixing operation in Figure 12 should then be chosen as,

$$f_l = f_c - f_{c,u} = f_c - (N_g + \frac{K-1}{2})f_\Delta \quad (7.18)$$
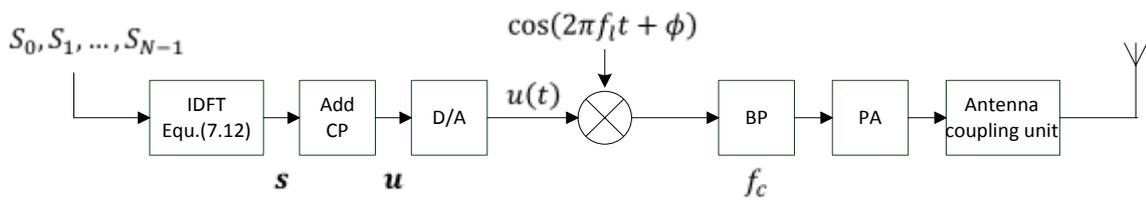
Figure 12. Illustrating how to create the OFDM signal $u(t)$ in Equation (7.15). The size-N IDFT in Equation (7.12) is used and N is given by Equation (7.4). The construction of the sequence $S_0, S_1, \dots, S_{N-1}$ is given by Equations (7.10)-(7.11). This figure also includes a possible frequency up-conversion to a higher carrier frequency f_c. The band-pass (BP) filter is then centered around f_c, and PA means the power amplifier.

The requirements on the band-pass filter in Figure 12 can be somewhat relaxed due to the parameter N_g, since this parameter gives a guard band in the frequency domain equal to $2N_g f_\Delta$ Hz that separates the lower sideband from the desired upper sideband (which is the up-modulated OFDM signal).

As an **example** consider an OFDM signal $u(t)$ with the parameters: K=420, $N_g = 20$, and $f_\Delta = 4$ kHz. The values of the sub-carrier frequencies f_0 and f_{K-1} then equals $f_0 = 80$ kHz and $f_{K-1} = 1.756$ Mhz. In this case N should be chosen larger than 880. If N is chosen to be N=1024 then the sampling frequency 4.096 MHz is used, and $N_x = 145$.

A short summary of some basic relationships in Section 7:

- N time-domain real samples of the real OFDM signal are specified in Equation (7.6).
- The size-N input sequence to the IDFT, i.e. the frequency-domain samples obtained from the DFT are given by Equations (7.10)-(7.11) (the remaining N-2K samples are equal to zero).
- Observe the importance of Equation (7.12), since the output sequence from the IDFT is the sequence of time-domain real samples specified by Equation (7.6). See also Figure 12.
- Equation (7.13) specifies the size-(L+N) vector of time-domain real samples that represents the entire OFDM signal interval (i.e. including the CP).
- The cyclic prefix is represented by the first L time-domain samples, see also Equation (7.14).
- Observe the importance of Equation (7.15), and the transmitter implementation in Figure 12.

Section 8: An alternative receiver implementation

In this section we will study an alternative implementation of the receiver that is possible if the sampling frequency is approximately at least twice as high than the sampling frequency used in Section 6 (where $f_{samp} = Nf_\Delta > Kf_\Delta$) if the same K and f_Δ are used. A higher sampling frequency normally implies a higher cost, e.g., for A/D converters. However, as we will see, interesting and useful alternative implementations can then be obtained.

In this section it is assumed that *at a certain stage in the receiver* the real noisy OFDM signal $r(t)$ is available where,

$$r(t) = u_r(t) + w(t) \tag{8.1}$$

In Equation (8.1) the signal $u_r(t)$ denotes the noise-free part of $r(t)$, and it is assumed that the received real OFDM signal $u_r(t)$ here can be expressed as,

$$u_r(t) = Re\left\{\sum_{k=0}^{K-1} a_k H_{eq,k} e^{j2\pi f_k(t-T_{CP})}\right\}, \qquad T_{CP} \le t \le T_s \tag{8.2}$$

where the different sub-carrier frequencies are,

$$f_k = (N_g + k)f_\Delta \qquad\qquad n = 0,1,...,K-1 \tag{8.3}$$

The sub-carrier frequencies f_k here have relatively low frequencies, since N_g ($N_g \ge 1$) is an integer design parameter of the receiver assumed to have a relatively small value.

Similar to Section 6 the "equivalent channel" parameter $H_{eq,k}$ in Equation (8.2) represents the combined effect, associated with sub-carrier frequency f_k, of sub-blocks in the communication chain, compare with Equation (6.16). Since $H_{eq,k} = |H_{eq,k}|e^{jarg(H_{eq,k})}$ the phase $arg(H_{eq,k})$ may also include (absorb) a phase-component that is a consequence of the specific description of $u_r(t)$ used in Equation (8.2).

The signal $w(t)$ in Equation (8.1) represents band-limited (low-pass) additive "white" Gaussian noise within the bandwidth of $u_r(t)$, i.e. within the approximate frequency range $|f| \le (N_g + K)f_\Delta$.

Observe that the description of $u_r(t)$ in Equation (8.2) is independent of the particular implementation method used at the transmitter side when implementing the transmitted OFDM signal.

We now want to obtain a sampled version of the real signal $r(t)$. Using the same arguments that was used in step 2 in Section 2, we conclude that the ***sampling frequency*** f_{samp} can be chosen as $f_{samp} = Nf_\Delta$ samples per second, and

$$f_{samp} = Nf_\Delta > 2(N_g + K)f_\Delta \tag{8.4}$$

and large enough such that the sampling theorem ([1]) is sufficiently fulfilled. Hence, the sampling frequency in this section is approximately ***at least twice as high*** as in Section 6 (for the same values of K and f_Δ).

Note that the choice of N to use in the receiver is a decision of the *engineers of the receiver*, and it does ***not*** need to be the same value as was chosen at the transmitter side (which typically also is unknown in many cases).

Corresponding to the current OFDM interval $0 \leq t \leq T_s$, the sequence of real time-domain samples generated from the A/D converter in Figure 13 below is $r(mT_{obs}/N), m = 0,1,\dots,(L+N-1)$.

Note however that the first L samples (the CP) will usually not be used in the detection process and these samples are therefore **removed**. This means that the signal interval where an overlap between OFDM signals may occur is ignored by the receiver, and thereby possible inter-symbol interference between OFDM signals is eliminated in the receiver (provided that $T_{ch} \leq T_{CP}$), see also Section 5. Since the CP is assumed to be much smaller than T_s, the loss of ignoring the CP is here assumed to be acceptable.

The remaining N samples are extremely important and they are collected in the real vector $\mathbf{r}$ having elements r_n defined by,

$$r_n = r((L+n)T_{obs}/N), \quad n = 0,1,\dots,N-1 \tag{8.5}$$

From Equations (8.1)-(8.2) it is concluded that the discrete-time signal $\mathbf{r}$, see also Figure 13, is a sampled version of the signal $x_r(t)$, where $x_r(t)$ is,

$$x_r(t) = r(t + T_{CP}) = Re\left\{\sum_{k=0}^{K-1} a_k H_{eq,k} e^{j2\pi f_k t}\right\} + w'(t), \qquad 0 \leq t \leq T_{obs} \tag{8.6}$$
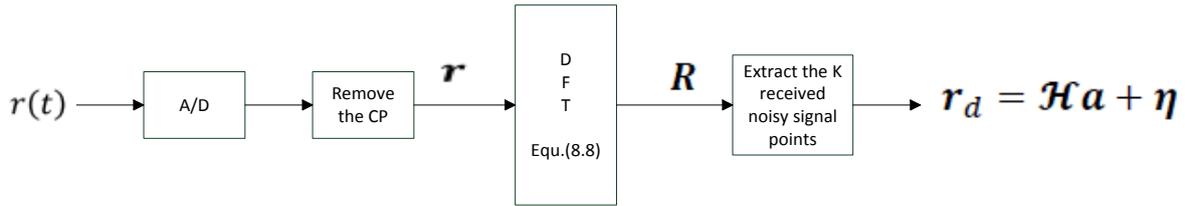
Figure 13. Illustrating a possible way to extract the K received distorted and noisy signal points. The real noisy OFDM signal $r(t)$ is given by Equations (8.1)-(8.3), and it is assumed to be available at a certain stage in the receiver. The size-N DFT in Equation (8.8) is used and N is given by Equation (8.4). The final desired result $\mathbf{r}_d$ is given in Equations (8.12)-(8.13).

Using the DFT:

The remaining investigation of the receiver aims to find the K received distorted and noisy signal points. To efficiently obtain these signal points with the size-N DFT, let us continue as follows.

Consider the Fourier transform of the real discrete-time signal $\mathbf{r}$ in Equation (8.5),

$$R(v) = \sum_{n=0}^{N-1} r_n e^{-j2\pi vn} \tag{8.7}$$

Remember from, e.g., Figure 4 on page 14 that $R(v)$ is periodic in v with period 1. Note however that $R(v)$ in Equation (8.7) exhibit symmetries since the time-domain samples in $\mathbf{r}$ are real. Furthermore, the Fourier transform of the signal $x_r(t)$ in Equation (8.6) appears as a very significant part of $R(v)$ within the fundamental interval $-1/2 \leq v \leq 1/2$, see Equation (2.17) on page 14 and the example in connection to Figure 5 on page 15.

As has already been mentioned the K received distorted and noisy signal points can be obtained by calculating the Fourier transform of the signal $x_r(t)$ in Equation (8.6) at K specific frequencies, i.e. by *sampling the Fourier transform* at K specific frequencies. ***Since the DFT results in frequency-domain samples it is very well suited for extracting the desired signal points***.

Let us therefore calculate the size-N **DFT** of the discrete-time signal r,

$$R_m = R(v = m/N) = \sum_{n=0}^{N-1} r_n e^{-j2\pi mn/N}, \quad m = 0,1,...,N-1 \tag{8.8}$$

In practice, **N is chosen as a power of 2** since fast Fourier transform (FFT) algorithms can then be used to significantly speed up the calculations in Equation (8.8).

In Figure 13 on the previous page the size-N column vector R contains the frequency-domain samples R_m.

The frequency-domain sample R_m is obtained at the normalized frequency

$$v = \frac{m}{N} = \frac{mf_\Delta}{Nf_\Delta} \tag{8.9}$$

We can now write R as,

$$R = X_r + w_r \tag{8.10}$$

where X_r is the noise-free part of R, and w_r is the noise vector. The element with index m in the vector X_r is denoted $X_{r,m}$.

By comparing the signal $s(t)$ in Equation (7.3) with the signal $x_r(t)$ in Equation (8.6), it is concluded from the result in Equation (7.10) that the sequence of K values $X_{r,N_g}, X_{r,N_g+1}, ..., X_{r,N_g+K-1}$ is identical with the sequence of values $(Na_0 H_{eq,0}, Na_1 H_{eq,1}, ..., Na_{K-1} H_{eq,K-1})$.

The desired received distorted and noisy signal points, denoted $r_{d,k}$, are thereby found since,

$$r_{d,k} = \frac{1}{N} R_{N_g+k} = a_k H_{eq,k} + \frac{1}{N} w_{r,N_g+k} \quad , k = 0,1,...,K-1 \tag{8.11}$$

This fundamental result can be expressed in the same way as in Section 6,

$$r_d = \mathcal{H}a + \eta \tag{8.12}$$

where the elements in the size-K column vector r_d are the desired received distorted and noisy signal points,

$$r_{d,k} = a_k H_{eq,k} + \eta_k, \quad k = 0,1,...,(K-1) \tag{8.13}$$

where η_k denotes additive complex Gaussian noise.

The results in Equations (8.12)-(8.13) are extremely important**!** See also Figure 13 on the previous page. Note that these results have the same form as the corresponding results that was obtained in Section 6.

The next step in the receiver is to feed the vector r_d to the decoding unit (compare with Figure 2 on page 2). However, decoding algorithms are not covered in these lecture notes.

This concludes these lecture notes where an introduction to OFDM has been given. Examples of IDFT-based implementations at the transmitter side, and DFT-based implementations at the receiver side have been the focus of these lecture notes.

A short summary of some basic relationships in Section 8:

- Observe the assumptions given by Equations (8.1)-(8.3).
- The sampling frequency is specified in Equation (8.4).
- Figure 13 on page 52 illustrates sampling, removal of the CP, and the size-N DFT. The input sequence to the DFT contains N time-domain real samples that corresponds to the observation interval of the receiver.
- After removal of the CP, the relationships defined by Equations (8.5)-(8.6) are obtained.
- The size-N DFT output sequence can be described by Equation (8.10). See also the text that follows this equation. Equation (8.11) shows how the desired signal points are obtained from the frequency-domain samples.
- The final desired result is obtained in Equations (8.12)-(8.13), see also Figure 13. This result, i.e. the K complex values in the vector r_d, is extremely important and it is delivered to the decoding unit.

References

[1] J. G. Proakis, D. G. Manolakis, *Digital Signal Processing, Principles, Algorithms and Applications*, Third Edition, Prentice Hall, 1996.

[2] J. G. Proakis, M. Salehi, *Digital Communications*, Fifth Edition, McGraw-Hill, 2008.

[3] D. Tse, P. Viswanath, *Fundamentals of Wireless Communication*, Cambridge University Press, 2005.

[4] A. Goldsmith, *Wireless Communications*, Cambridge University Press, 2005.

[5] M. Schwarts, *Mobile Wireless Communications*, Cambridge University Press, 2005.

[6] A. R. S. Bahai, B. R. Saltzberg, M. Ergen, *Multi-Carrier Digital Communications, Theory and Applications of OFDM*, Second Edition, Springer Science+Business Media, Inc, 2004.

[7] Y. Li, G. L. Stüber, *Orthogonal Frequency Division Multiplexing for Wireless Communications*, Springer Science+Business Media, Inc, 2006.

[8] R. Van Nee, R. Prasad, *OFDM for Wireless Multimedia Communications*, Artech House, 2000.

[9] E. Dahlman, S. Parkwall, J. Sköld, *4G LTE/LTE-Advanced for Mobile Broadband*, Second Edition, Academic Press, 2014.

[10] J. Li, X. Wu, R. Laroia, *OFDMA Mobile Broadband Communications, A Systems Approach*, Cambridge University Press, 2013.

[11] E. Perahia, R. Stacey, *Next Generation Wireless LANs. Throughput, Robustness, and Reliability in 802.11n,* Cambridge University Press, 2008.